HEP seminar (via Skype) at IIT Hyderabad,
28 Feb. 2019

Gravitational lensing by exotic objects

Hideki Asada

弘前大学
Hirosaki University

MEXT(No. 17H06359)

JSPS(No. 17K05431)

Main reference:

HA, Mod. Phys. Lett. A, 32, 1730031 (2017)
for a brief review on “GL by exotic objects”

See also a book “Lorentzian Wormholes” (Matt Visser)

Outline

1. Black Holes (BHs) and Wormholes (WHs)

2. Gravitational Lensing by BHs

3. Gravitational Lensing by WHs

4. Gravitational lensing by an exotic object:

--- as a probe of new physics

1. Black Holes (BHs) and Wormholes (WHs)

BHs (candidates) are real and astrophysical objects by EM(X-ray) and GW methods

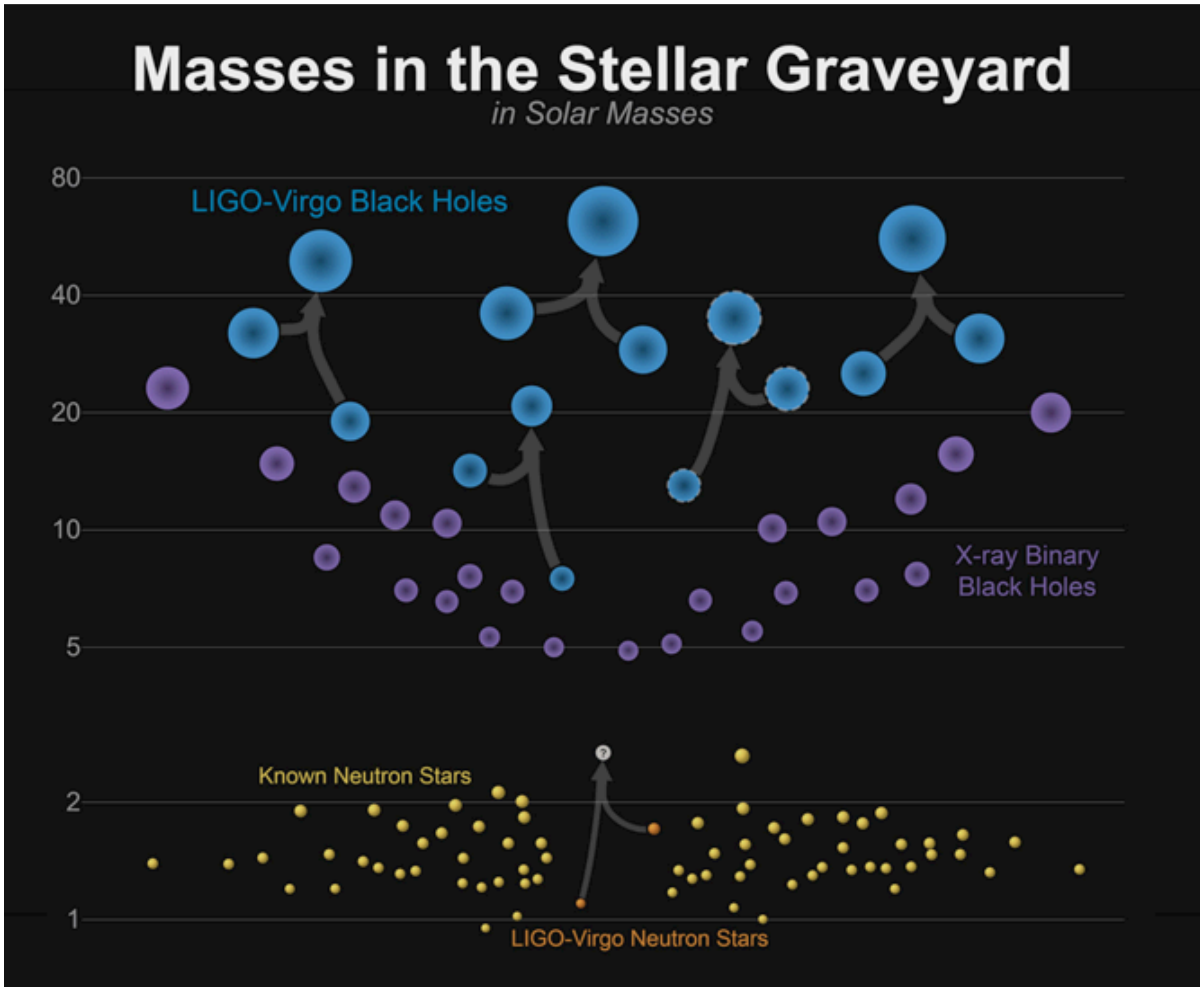

BHs

Horizon is caused by strong gravity (pull)

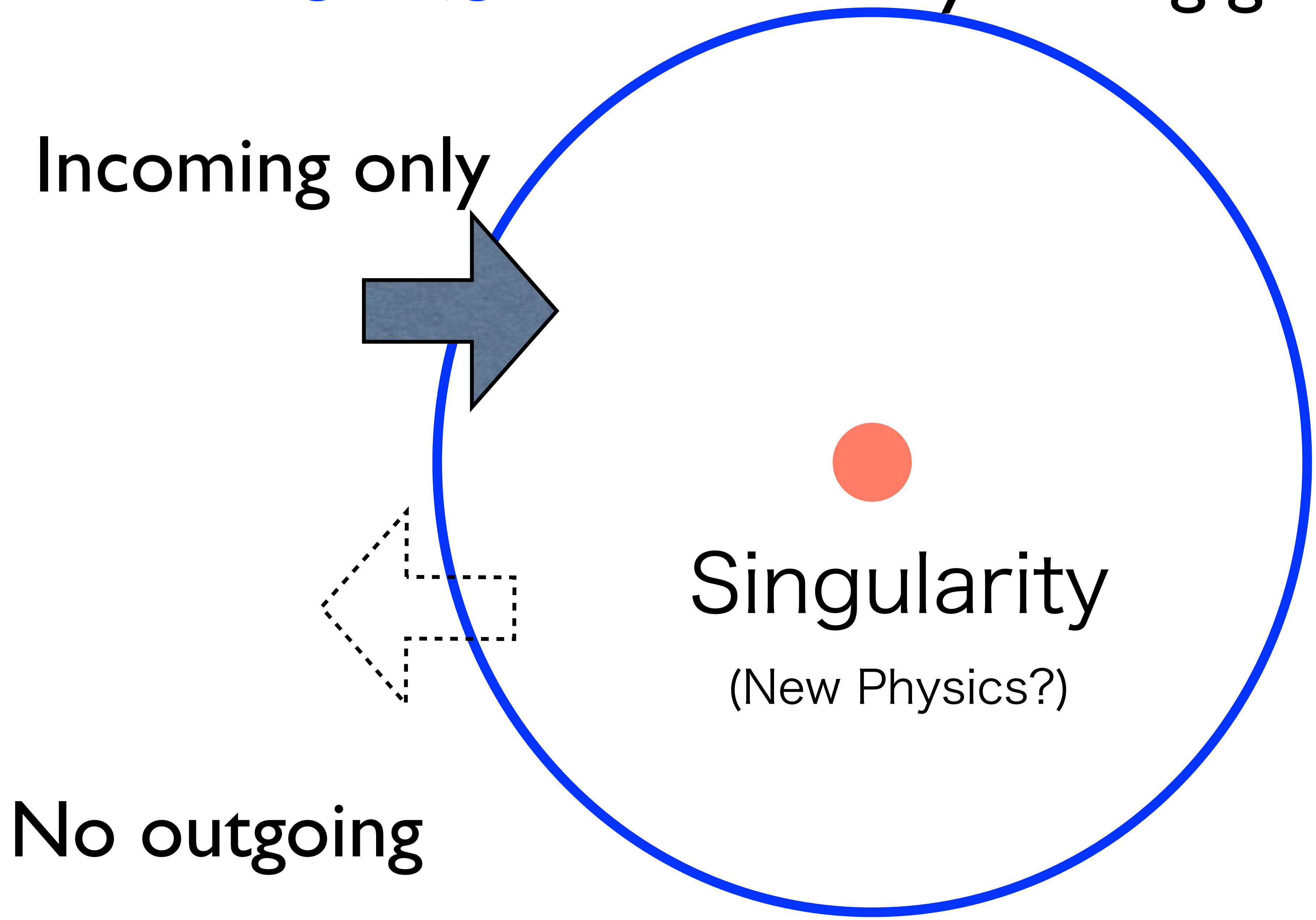

Wormholes (WHs) coined by John Wheeler (1957)

a spacetime “tunnel”

Speculative objects connecting two different points in a spacetime

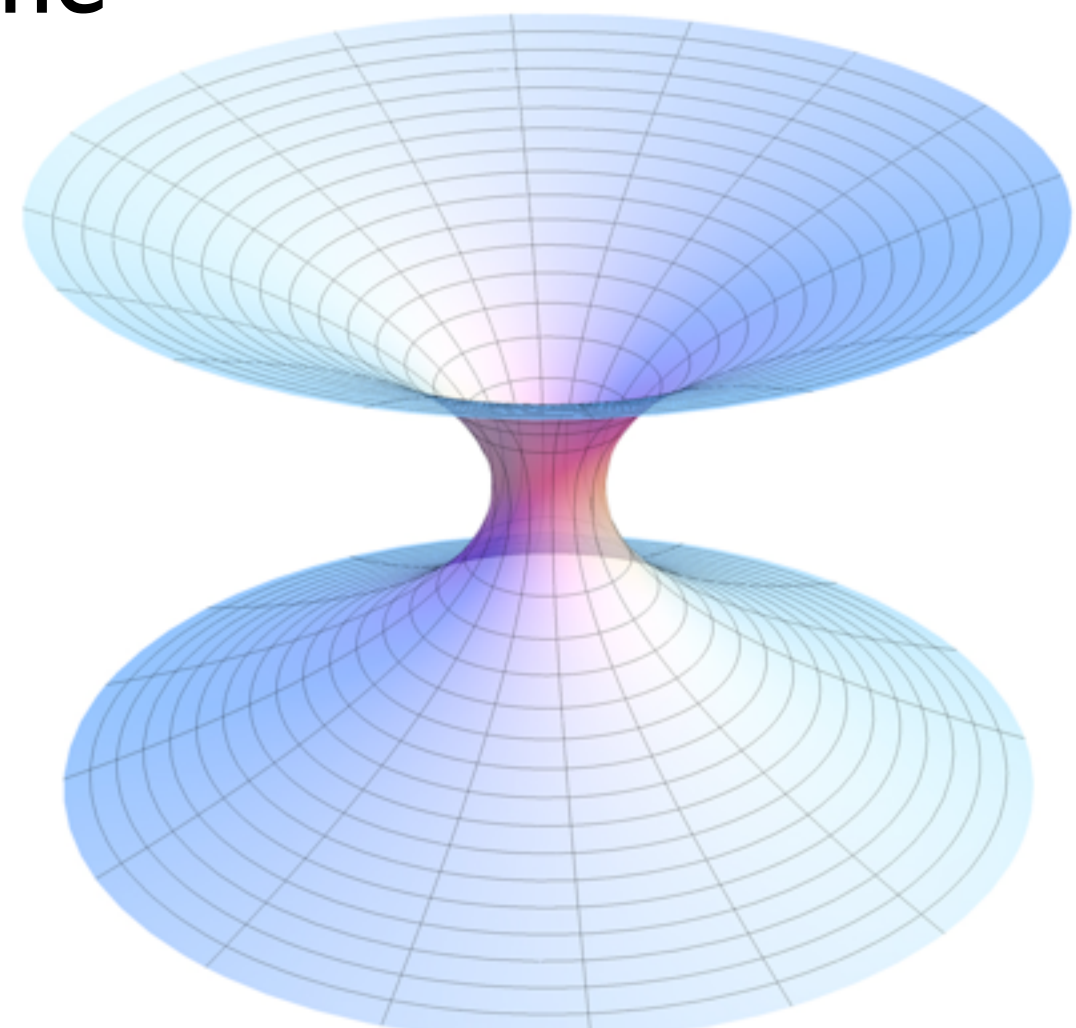

non-trivial topology (non-simply connected)

WHs require a violation of some energy conditions (in GR)

or a modification of gravity theories.

e.g.

Null Energy Condition (NEC):

For any null vector, $$T_{\mu\nu}k^{\mu}k^{\nu} \geq 0$$

Averaged Null Energy Condition (ANEC):

On a null curve, $$\int_{\Gamma} T_{\mu\nu}k^{\mu}k^{\nu}d\lambda \geq 0$$

On a construction of WHs (spacetime tunnels):

"Tidal fields" (in GR) are described by Raychaudhuri equation.

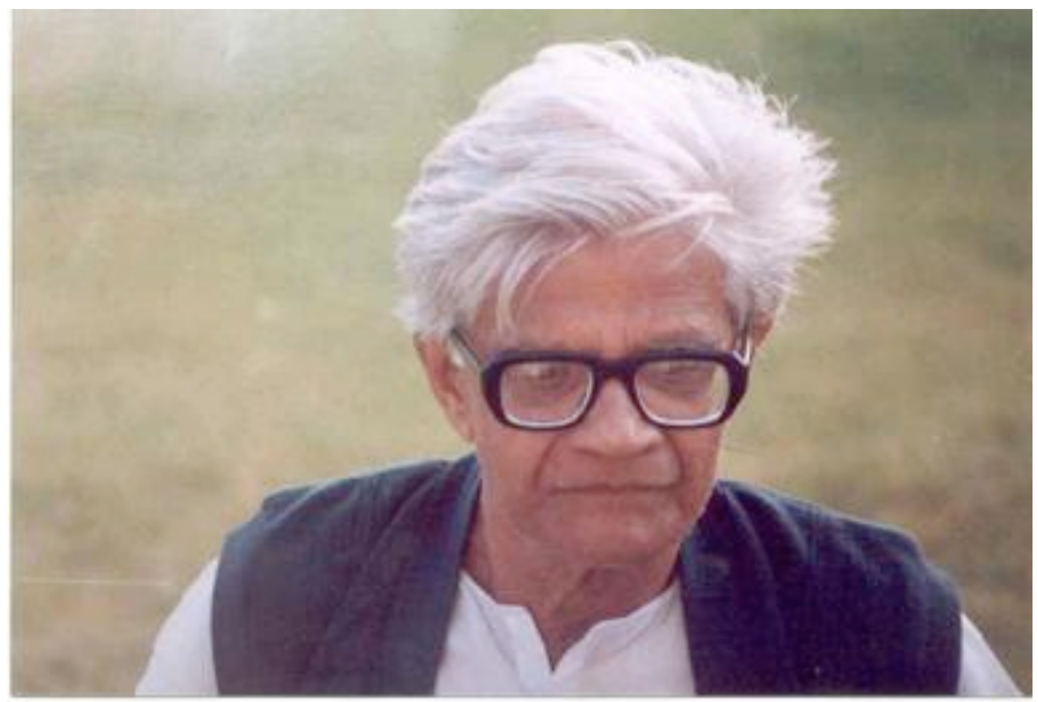

Amal Kumar Raychaudhuri (1923-2005)

Raychaudhuri equation for null geodesics

$$\frac{d\hat{\theta}}{d\lambda} = -R_{\mu\nu}k^{\mu}k^{\nu} - 2\hat{\sigma}^2 - \frac{1}{2}\hat{\theta}^2 + 2\hat{\omega}^2$$

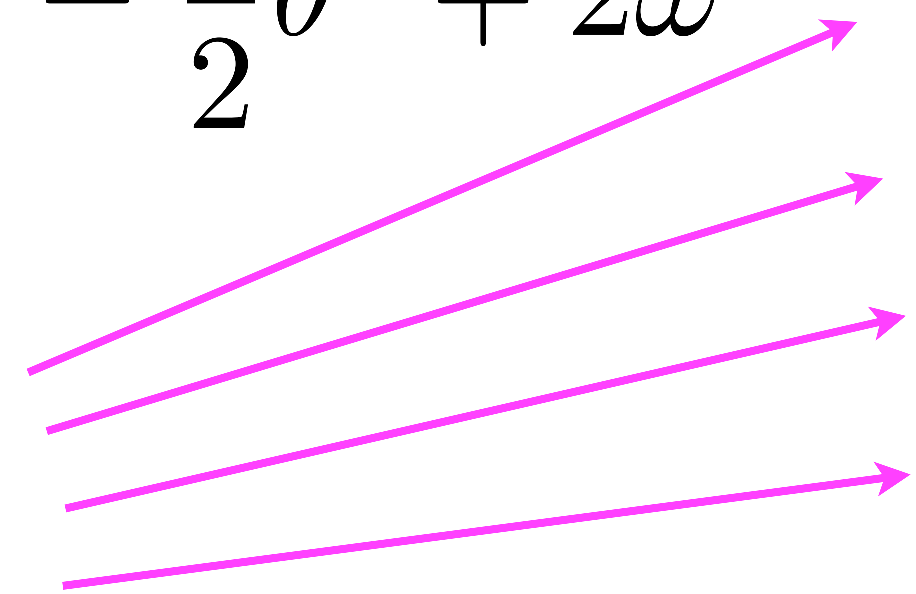

$$\hat{\theta} \equiv P^{\nu}{}_{\mu}(\nabla_{\nu}k^{\mu})$$

Expansion rate of null geodesic bundle

$$\hat{\sigma}_{\mu\nu} \equiv P^{\alpha}_{<\mu}P^{\beta}_{\nu>}\nabla_{\alpha}k_{\beta}$$

Shear of the bundle

$$\hat{\omega}_{\mu\nu} \equiv P^{\alpha}_{[\mu}P^{\beta}_{\nu]}\nabla_{\alpha}k_{\beta}$$

Vorticity of the bundle

(P^{α}_{μ} Projection tensor)

We consider the throat of a spherically symmetric WH.

For purely radial null geodesics,

$$\hat{\sigma}_{\mu\nu} = 0 \qquad \hat{\omega}_{\mu\nu} = 0$$

Then,

$$\frac{d\hat{\theta}}{d\lambda} = -R_{\mu\nu}k^{\mu}k^{\nu} - \frac{1}{2}\hat{\theta}^2$$

The minimal cross-section area of the null bundle occurs at the WH throat:

$$\hat{\theta} = 0 \qquad \& \qquad \frac{d\hat{\theta}}{d\lambda} \geq 0$$

Therefore, at the throat

$$R_{\mu\nu}k^{\mu}k^{\nu} \leq 0$$

By using Einstein equation (in GR), this is rewritten as

$$T_{\mu\nu}k^{\mu}k^{\nu} \leq 0$$

Null energy condition must be violated at the throat.

N.B.

By integrating along the null geodesic, one can see that

averaged null energy condition must be violated in WHs.

2. Gravitational Lensing by BHs (and stars)

Gravitational Microlensing

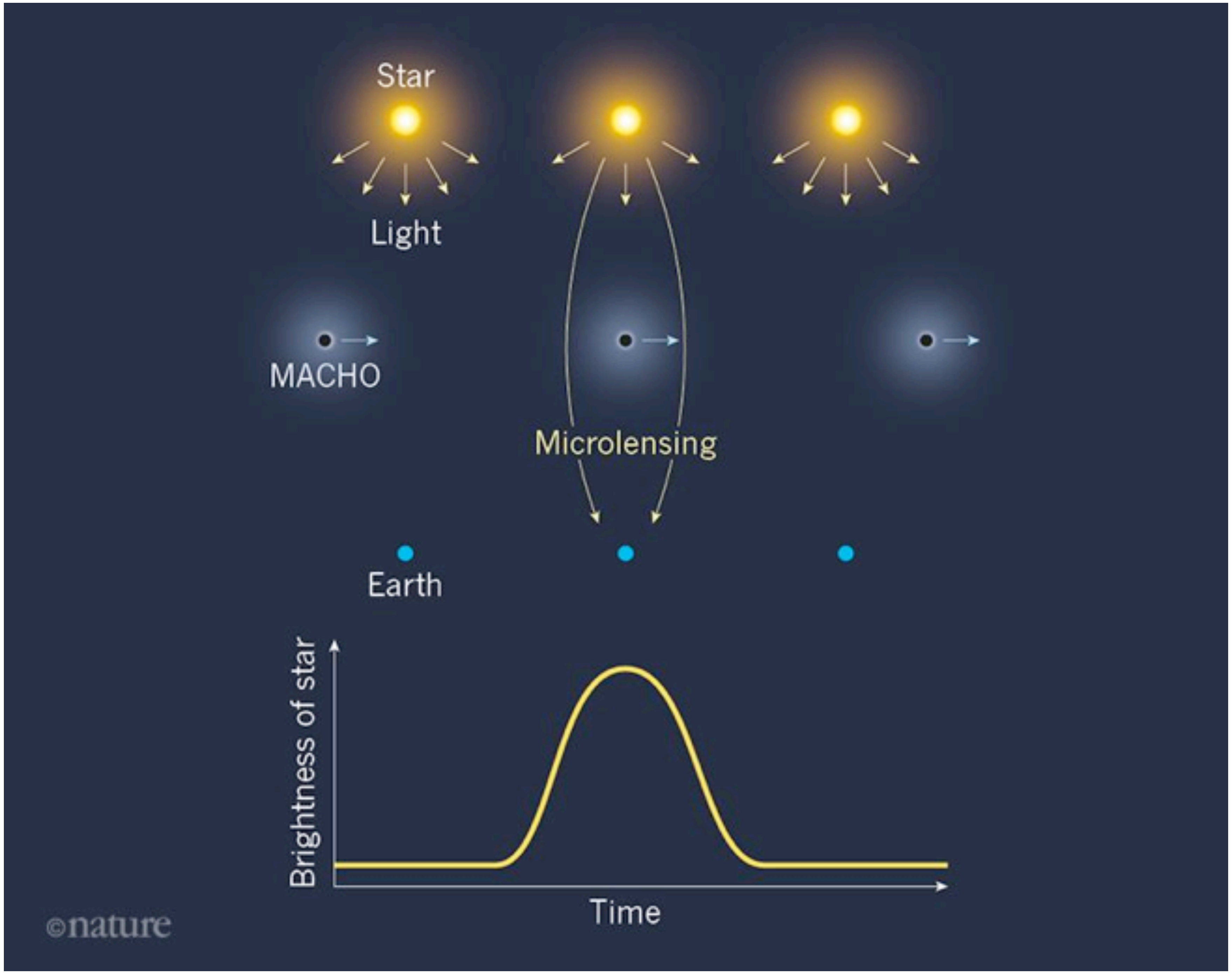

Light deflection

$$\frac{4GM}{c^2 b}$$

Nature, 562, 349 (2018)

Stronger gravitational pull

More light rays

Brighter image

Microlensing by WHs ?

3. Gravitational Lensing by WHs

Light propagation in Ellis wormhole, especially deflection angle of light, is discussed by many authors.

[8] L. Chetouani and G. Clément, Gen. Relativ. Gravit. **16**, 111 (1984).

[9] G. Clément, Int. J. Theor. Phys. **23**, 335 (1984).

[10] V. Perlick, Phys. Rev. D **69**, 064017 (2004).

[11] M. Safonova, D. F. Torres, and G. E. Romero, Phys. Rev. D **65**, 023001 (2001).

[12] A. A. Shatskii, Astronomy Reports **48**, 525 (2004).

[13] K. K. Nandi, Y. Z. Zhang, and A. V. Zakharov, Phys. Rev. D **74**, 024020 (2006).

[14] F. Abe, Astrophys. J. **725**, 787 (2010).

[16] T. K. Dey and S. Sen, Mod. Phys. Lett. A **23**, 953 (2008).

[17] A. Bhattacharya and A. A. Potapov, Mod. Phys. Lett. A **25**, 2399 (2010).

[19] K. Nakajima and H. Asada, Phys. Rev. D **85**, 107501 (2012).

[20] G. W. Gibbons and M. Vyska, Classical Quantum Gravity **29**, 065016 (2012).

PHYSICAL REVIEW D **85,** 107501 (2012)

Deflection angle of light in an Ellis wormhole geometry

Koki Nakajima and Hideki Asada
Faculty of Science and Technology, Hirosaki University, Hirosaki 036-8561, Japan
(Received 1 March 2012; published 3 May 2012)

Dey and Sen (2008) formula

$$\alpha = \pi \left\{ \sqrt{\frac{2(r_0^2 + a^2)}{2r_0^2 + a^2}} - 1 \right\},$$

The correct one is derived as

(Perlick, Gibbons and Vyska, Nakajima and HA)

$$\alpha(b) = 2\int_0^1 \frac{dt}{\sqrt{(1-t^2)(1-k^2t^2)}} - \pi = 2K(k) - \pi, \tag{9}$$

where $t \equiv b/R$ and $k \equiv a/b$. The integral in Eq. (9) is a complete elliptic integral of the first kind $K(k)$, which admits a series expansion for $k < 1$. Hence, Eq. (9) is expanded as

$$\alpha(b) = \pi \sum_{n=1}^{\infty} \left[\frac{(2n-1)!!}{(2n)!!} \right]^2 k^{2n}. \tag{10}$$

Class. Quantum Grav. **29** (2012) 065016 (19pp) doi:10.1088/0264-9381/29/6/065016

The application of Weierstrass elliptic functions to Schwarzschild null geodesics

G W Gibbons[1,2] and M Vyska[2]

$$\frac{\delta\phi}{\pi} = -\frac{1}{4}\mu^2 - \frac{1}{2}\mu^3 - \frac{41}{64}\mu^4 - \frac{9}{16}\mu^5 - \frac{25}{256}\mu^6 + \frac{37}{128}\mu^7 + \frac{11\,959}{16\,384}\mu^8 + \frac{1591}{2048}\mu^9 + \frac{13\,311}{65\,536}\mu^{10} - \frac{29\,477}{32\,768}\mu^{11} - \cdots. \qquad (139)$$

Model

Ellis WH(1973)

$$ds^2 = dt^2 - dr^2 - (r^2 + \underline{a}^2)(d\theta^2 + \sin^2(\theta)d\phi^2), \qquad (1)$$

throat radius

Deflection angle of light in weak field

$$\alpha(r) \rightarrow \frac{\pi}{4}\frac{a^2}{r^2} - \frac{5\pi}{32}\frac{a^4}{r^4} + o\left(\frac{a}{r}\right)^6. \qquad (3)$$

($\frac{4M}{r}$ for BHs)

What is an astronomical implication by the different deflection of light in WHs?

THE ASTROPHYSICAL JOURNAL, 725:787–793, 2010 December 10 doi:10.1088/0004-637X/725/

GRAVITATIONAL MICROLENSING BY THE ELLIS WORMHOLE

F. ABE
Solar-Terrestrial Environment Laboratory, Nagoya University, Furo-cho, Chikusa-ku, Nagoya 464-8601, Japan; abe@stelab.nagoya-u.ac.jp
Received 2010 February 21; accepted 2010 October 7; published 2010 November 19

ABSTRACT

A method to calculate light curves of the gravitational microlensing of the Ellis wormhole is derived in the weak-field limit. In this limit, lensing by the wormhole produces one image outside the Einstein ring and another image inside. The weak-field hypothesis is a good approximation in Galactic lensing if the throat radius is less than 10^{11} km. The light curves calculated have gutters of approximately 4% immediately outside the Einstein ring crossing times. The magnification of the Ellis wormhole lensing is generally less than that of Schwarzschild lensing. The optical depths and event rates are calculated for the Galactic bulge and Large Magellanic Cloud fields according to bound and unbound hypotheses. If the wormholes have throat radii between 100 and 10^7 km, are bound to the galaxy, and have a number density that is approximately that of ordinary stars, detection can be achieved by reanalyzing past data. If the wormholes are unbound, detection using past data is impossible.

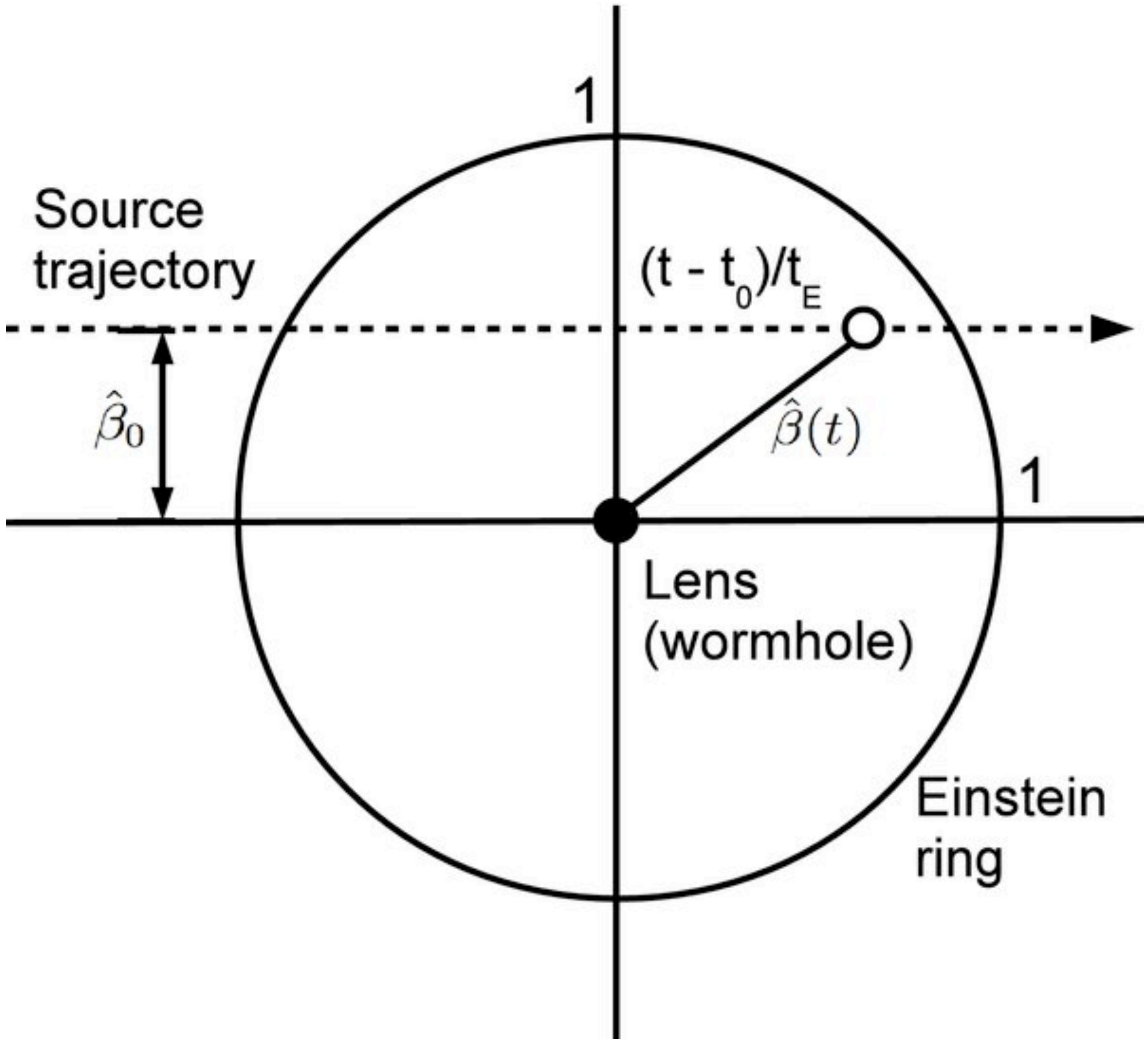
1
Source
trajectory
$(t - t_0)/t_E$
$\hat{\beta}_0$
$\hat{\beta}(t)$
1
Lens
(wormhole)
Einstein
ring

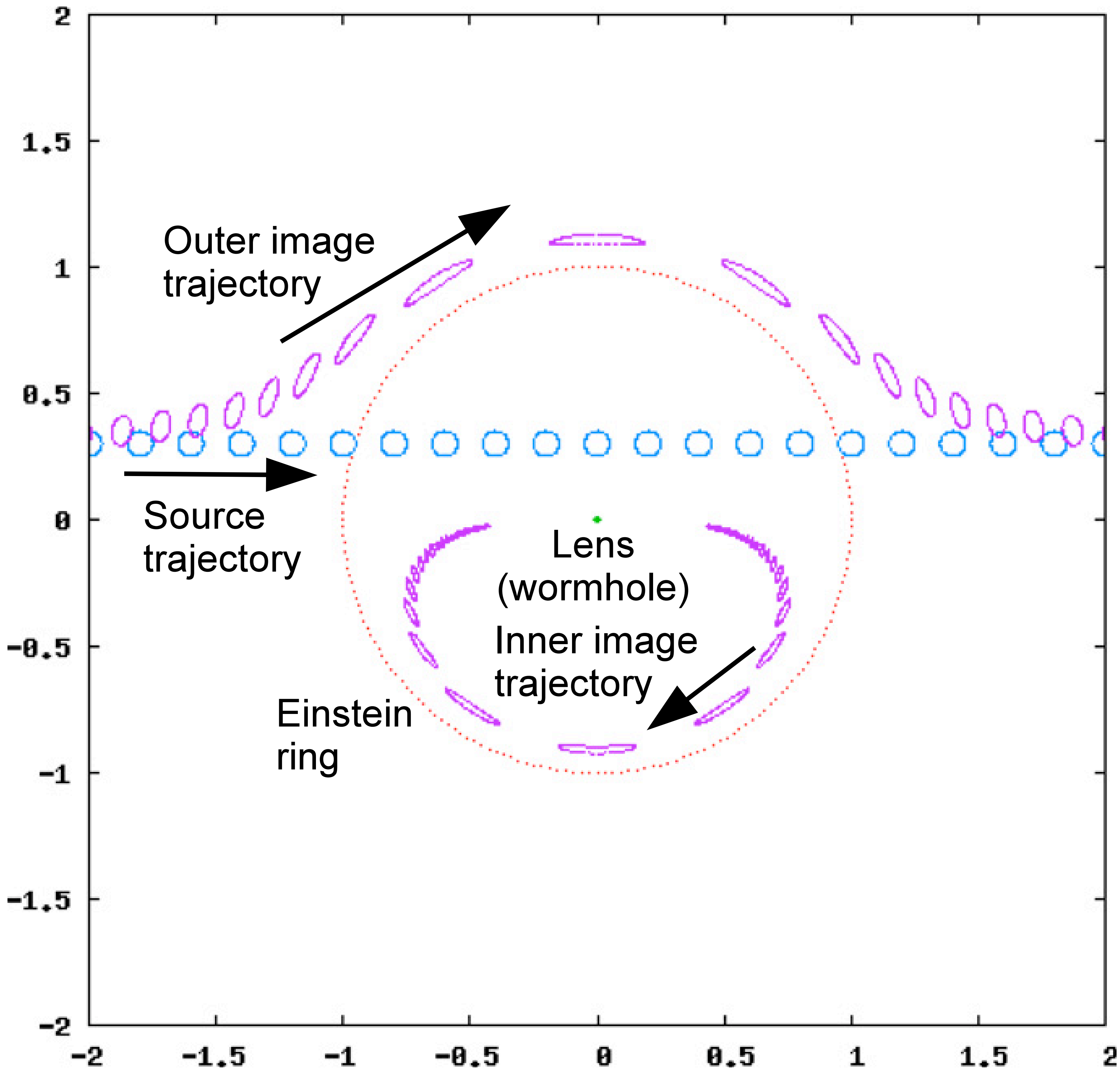

Outer image trajectory
Source trajectory
Lens (wormhole)
Inner image trajectory
Einstein ring
2
1.5
1
0.5
0
-0.5
-1
-1.5
-2
-2
-1.5
-1
-0.5
0
0.5
1
1.5
2

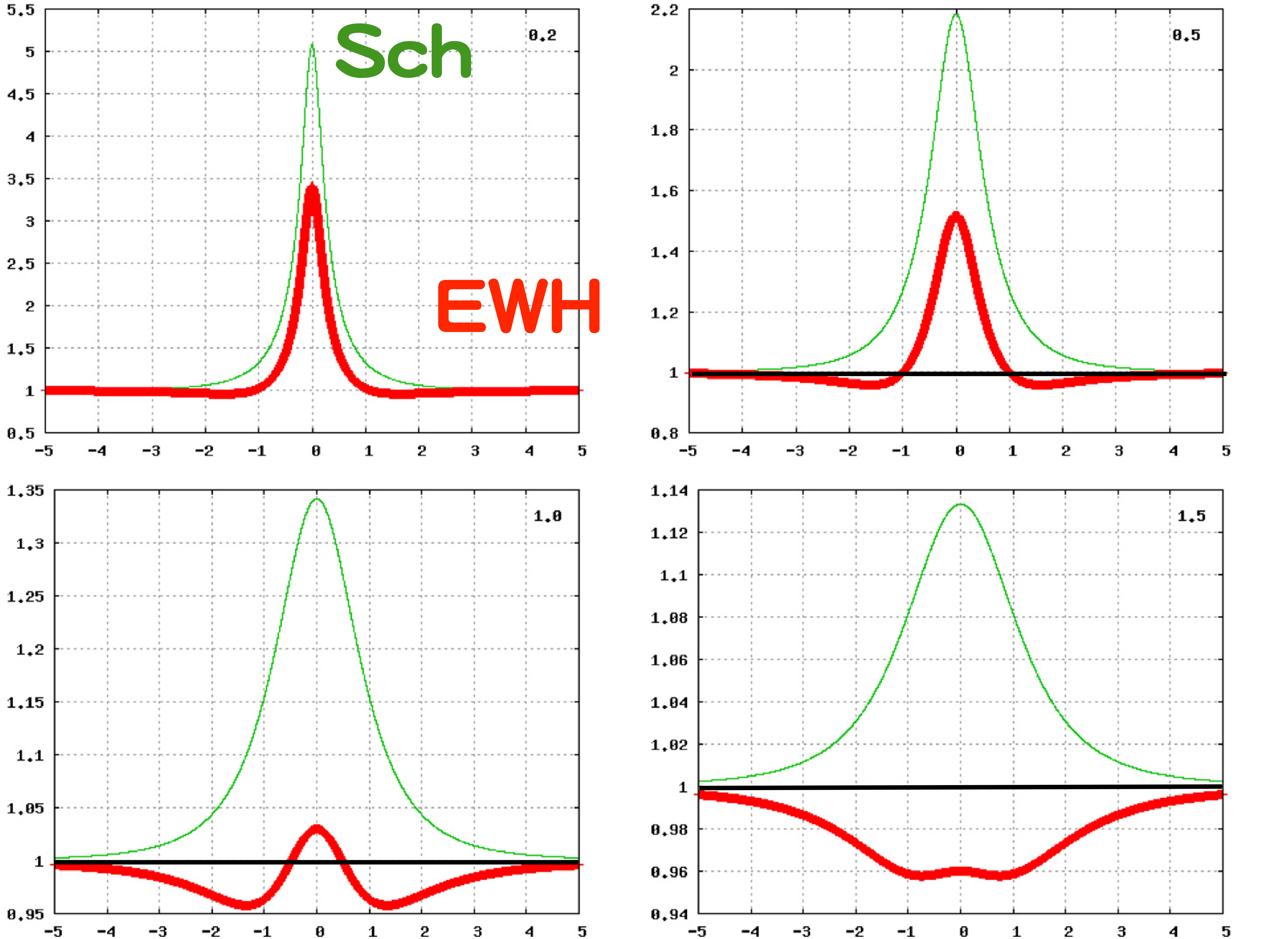

Figure 4. Light curves for $\hat{\beta}_0 = 0.2$ (top left), $\hat{\beta}_0 = 0.5$ (top right), $\hat{\beta}_0 = 1.0$ (bottom left), and $\hat{\beta}_0 = 1.5$ (bottom right). Thick red lines are the light curves for wormholes. Thin green lines are corresponding light curves for Schwarzschild lenses.

(A color version of this figure is available in the online journal.)

19年2月27日水曜日

Does this demagnification conclude wormholes?

To answer this, Kitamura, Nakajima, HA (2013)

we introduced a one-parameter model of a weak-field metric

Inverse power

$$ds^2 = -\left(1 - \frac{\varepsilon_1}{r^n}\right)dt^2 + \left(1 + \frac{\varepsilon_2}{r^n}\right)dr^2 + r^2(d\theta^2 + \sin^2\theta d\phi^2) + O(\varepsilon_1^2, \varepsilon_2^2, \varepsilon_1\varepsilon_2),$$

(1) static and asymptotically flat

(2) only in the weak field

(3) n=1 : Schwarzschild metric
n=2 : Ellis Worm Hole (EWH)

(4) n>1 : zero ADM mass (massless)

After a conformal transformation,

$$d\bar{s}^2 = -dt^2 + \left(1 + \frac{\varepsilon}{R^n}\right)dR^2 + R^2(d\theta^2 + \sin^2\theta d\phi^2) + O(\varepsilon^2),$$

where $\varepsilon \equiv n\varepsilon_1 + \varepsilon_2$ and

$$R^2 \equiv \frac{r^2}{(1 - \frac{\varepsilon_1}{r^n})}.$$

Deflection angle of light is calculated in the textbook manner as

$$\alpha = 2\int_{R_0}^{\infty} \frac{d\phi(R)}{dR} dR - \pi = \frac{\varepsilon}{b^n} \int_0^{\frac{\pi}{2}} \cos^n \psi \, d\psi + O(\varepsilon^2),$$

$$\begin{aligned}
\int_0^{\frac{\pi}{2}} \cos^n \psi \, d\psi &= \frac{(n-1)!!}{n!!} \frac{\pi}{2} (\text{even}\, n), \\
&= \frac{(n-1)!!}{n!!} (\text{odd}\, n), \\
&= \frac{\sqrt{\pi}}{2} \frac{\Gamma(\frac{n+1}{2})}{\Gamma(\frac{n+2}{2})} (\text{real}\, n > 0).
\end{aligned}$$

always positive constant

Deflection angle of light is written as

$$\alpha(b) = \bar{\varepsilon}/b^n$$

n=0 : Singular Isothermal Sphere (SIS)

n=1 : Stars and BHs

n=2 : Ellis Worm Hole (EWH)

This one-parameter model is used by Tsukamoto and Harada (2012, 2013).

How exotic is this lens model?

In the standard lens theory (in GR),
convergence (surface mass density) is

$$\kappa(b) = \frac{\bar{\varepsilon}(1-n)}{2} \frac{1}{b^{n+1}}$$

If ε>0 and n>1, negative convergence

(divergent "lens")

Analogy to opical lenses ---

convex lens

concave lens

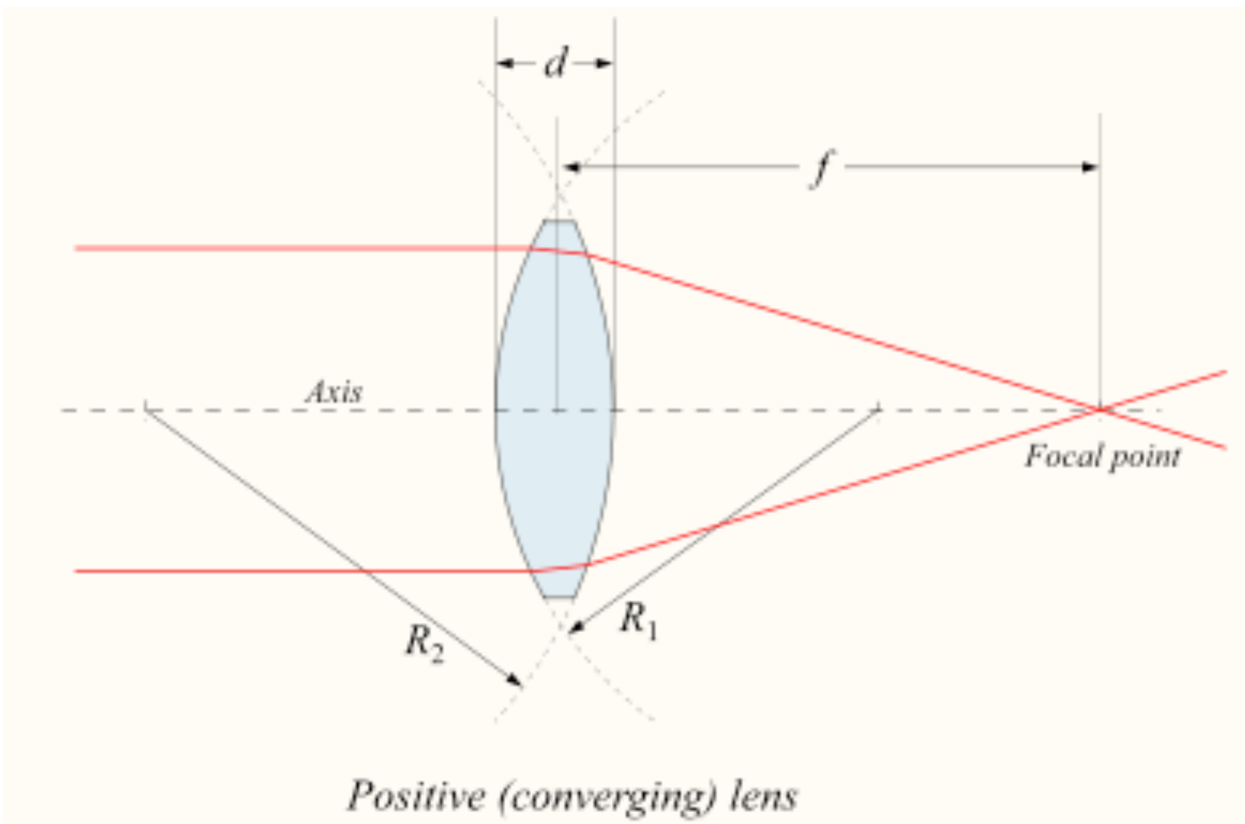

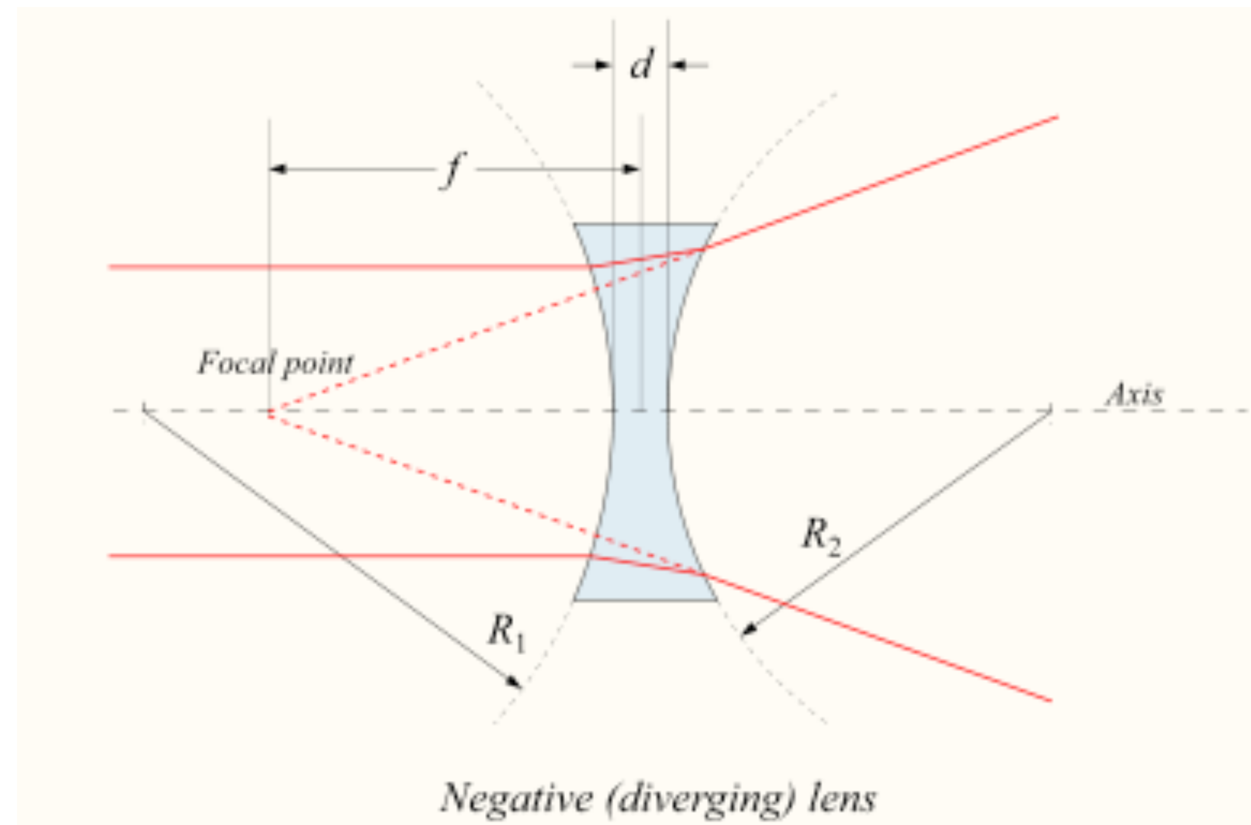

$$\kappa > 0 \qquad\qquad \kappa < 0$$

"Standard" Grav Lens "Diversing"

unusual

$\kappa > 0$ Non-vac. Ricci-focusing	$\varepsilon > 0$ & $n < 1$	SIS
	$\varepsilon < 0$ & $n > 1$	
Vac. $\kappa = 0$ Weyl-focusing	$n = 1$	Star&BH
$\kappa < 0$ Non-vac. Ricci-defocusing	$\varepsilon > 0$ & $n > 1$	EWH
	$\varepsilon < 0$ & $n < 1$	

Lens Equation with thin lens approx.

$$\beta = \frac{b}{D_L} - \frac{D_{\rm LS}}{D_S}\alpha(b),$$

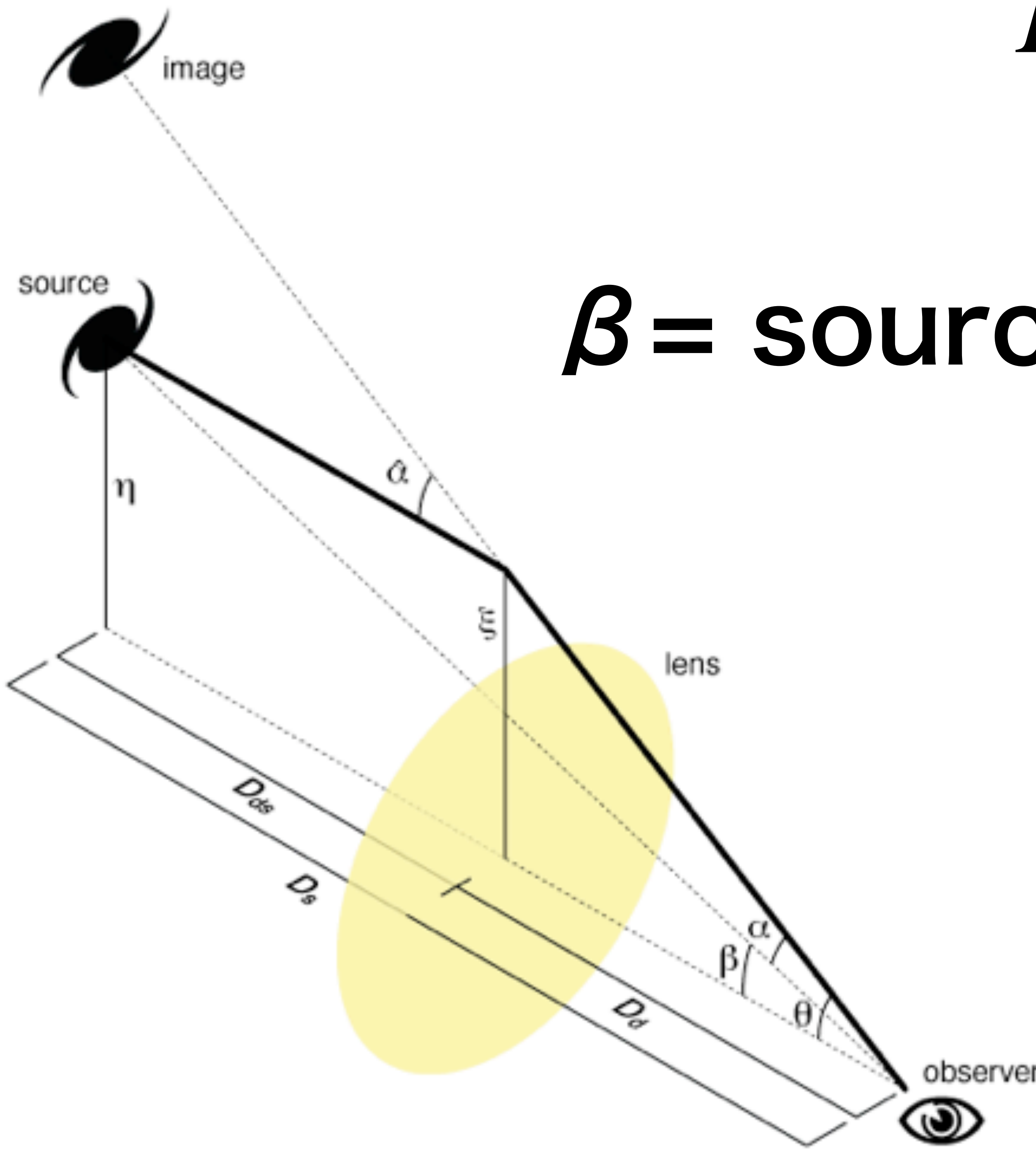

β = source angular position

If $\varepsilon < 0$,

repulsive

like a concave lens

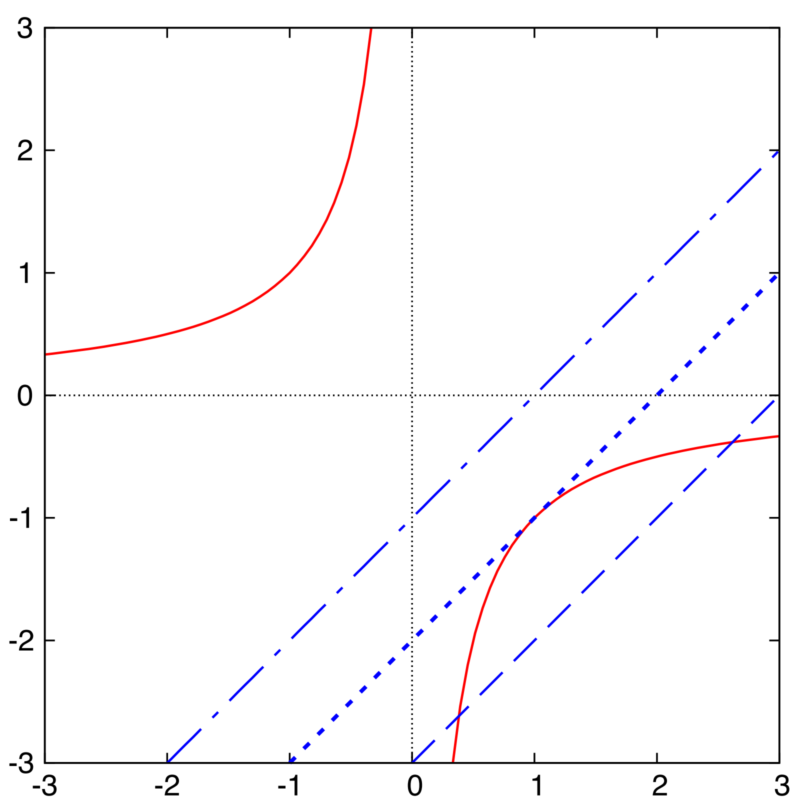

0 images

1 images

2 images

FIG. 3 (color online). Repulsive lens model ($\varepsilon < 0$). Solid curves denote $1/\hat{\theta}^n$ and straight lines mean $\hat{\theta} - \hat{\beta}$. Their intersections correspond to image positions that are roots for the lens equation. There are three cases: No image for a small $\hat{\beta}$ (dot-dashed line), a single image for a particular $\hat{\beta}$ (dotted line), and two images for a large $\hat{\beta}$ (dashed line). The two images are on the same side of the lens object.

For $\varepsilon > 0$,

Einstein ring for $\beta = 0$

$$\theta_{\mathrm{E}} \equiv \left(\frac{\bar{\varepsilon} D_{LS}}{D_S D_L^n}\right)^{\frac{1}{n+1}}.$$

If $\varepsilon < 0$,

(tentative) Einstein ring radius

$$\theta_{\mathrm{E}} \equiv \left(\frac{|\bar{\varepsilon}| D_{LS}}{D_S D_L^n}\right)^{\frac{1}{n+1}},$$

Three typical observables in GL

1) Image brightness (micro-lens)

2) Image shape (macro-lens)

3) Image motion (micro-lens)

1) Image brightness(micro)

PHYSICAL REVIEW D **87,** 027501 (2013)

Demagnifying gravitational lenses toward hunting a clue of exotic matter and energy

Takao Kitamura, Koki Nakajima, and Hideki Asada
Faculty of Science and Technology, Hirosaki University, Hirosaki 036-8561, Japan
(Received 3 November 2012; published 10 January 2013)

$\hat{\beta} \equiv \beta/\theta_E$ and $\hat{\theta} \equiv \theta/\theta_E$

$$\hat{\beta} = \hat{\theta} - \frac{1}{\hat{\theta}^n} \quad (\hat{\theta} > 0),$$

$$\hat{\beta} = \hat{\theta} + \frac{1}{(-\hat{\theta})^n} \quad (\hat{\theta} < 0),$$

For small beta (= source close to lens)

$$\hat{\theta}_{+} = 1 + \frac{1}{n+1}\hat{\beta} + \frac{1}{2}\frac{n}{(n+1)^2}\hat{\beta}^2 + O(\hat{\beta}^3) \quad (\hat{\theta} > 0), \tag{9}$$

$$\hat{\theta}_{-} = -1 + \frac{1}{n+1}\hat{\beta} - \frac{1}{2}\frac{n}{(n+1)^2}\hat{\beta}^2 + O(\hat{\beta}^3) \quad (\hat{\theta} < 0). \tag{10}$$

Axisymmetric along line of sight

A is $|(\beta/\theta) \times (d\beta/d\theta)|^{-1}$,

$$A_{\pm} = \frac{1}{\hat{\beta}(n+1)} + O(\hat{\beta}^0),$$

$$A_{\rm tot} \equiv A_+ + A_- = \frac{2}{\hat{\beta}(n+1)} + O(\hat{\beta}^0). \qquad (12)$$

Total demagnification (A_tot < 1), if

$$\hat{\beta} > \frac{2}{n+1}$$

under weak field, thin lens and small β approximations

Star and BH

EWH

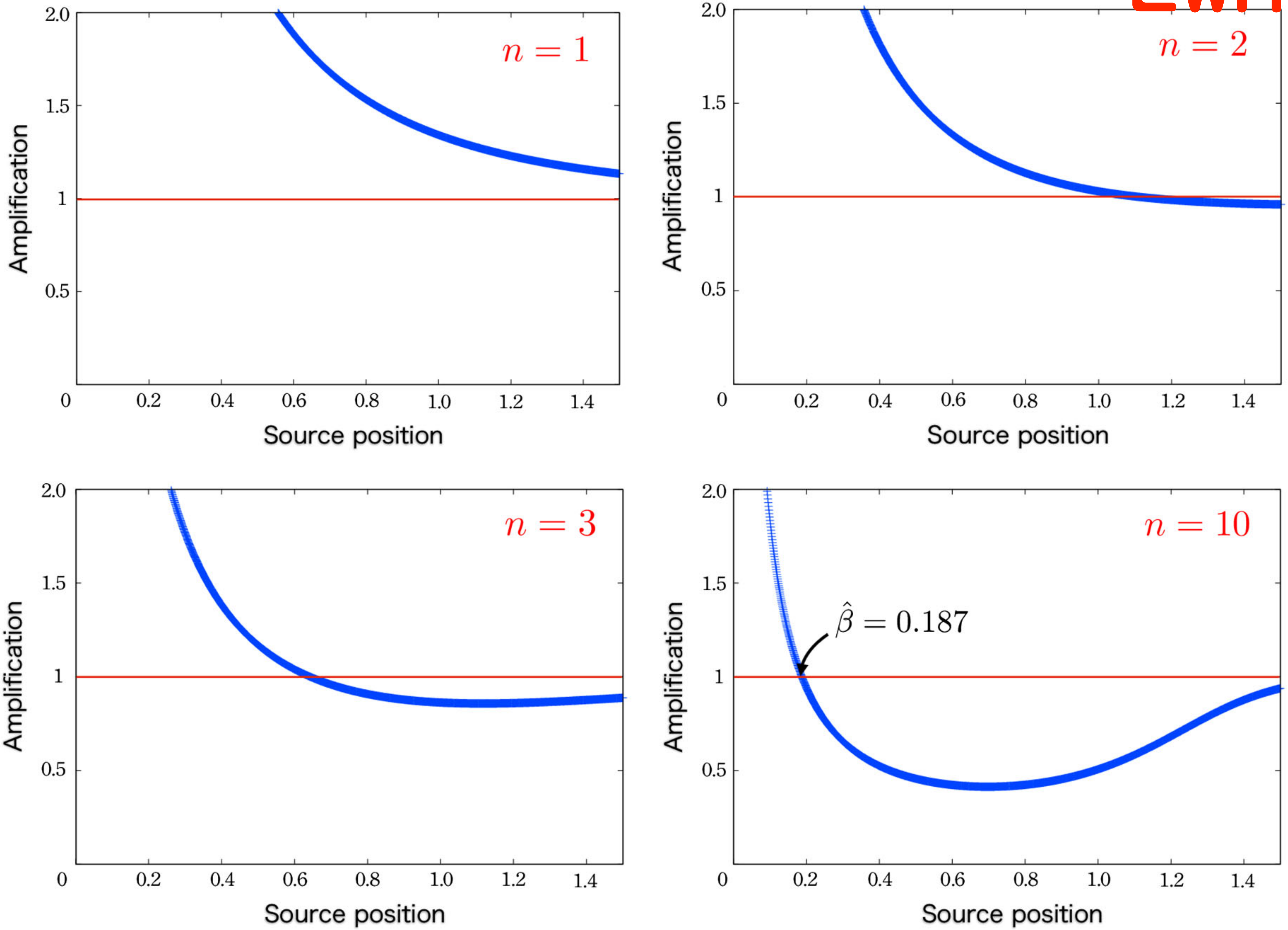

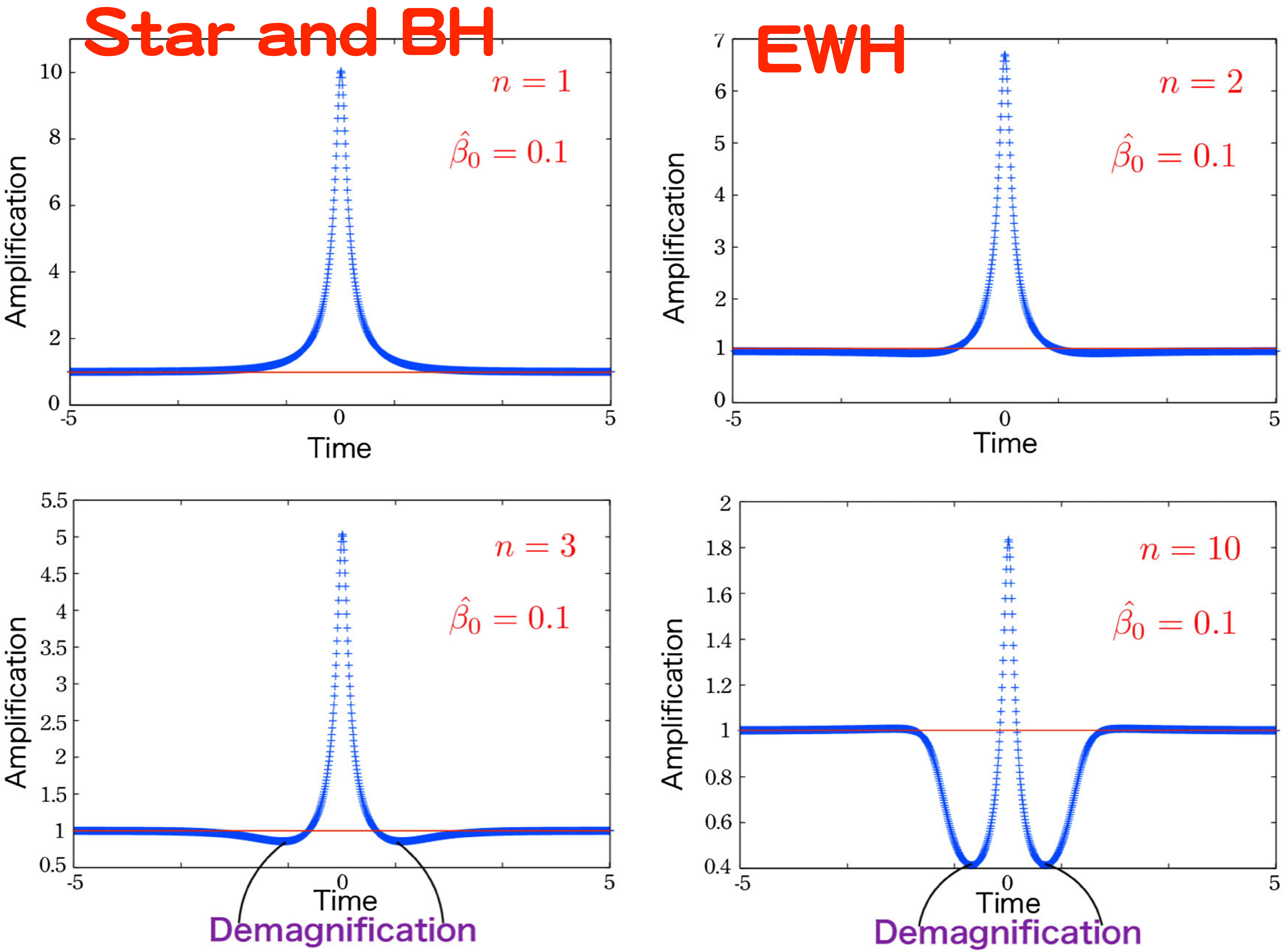

Star and BH
EWH
$n = 1$
$\hat{\beta}_0 = 0.1$
$n = 2$
$\hat{\beta}_0 = 0.1$
$n = 3$
$\hat{\beta}_0 = 0.1$
$n = 10$
$\hat{\beta}_0 = 0.1$
Amplification
Time
Demagnification
Demagnification

Time-symmetric demagnification
in light curves will be
an evidence for EWH (n=2)
but not a proof.

2) Image shape(macro)

PHYSICAL REVIEW D **88,** 024049 (2013)

Gravitational lensing shear by an exotic lens object with negative convergence or negative mass

Koji Izumi, Chisaki Hagiwara, Koki Nakajima, Takao Kitamura, and Hideki Asada
Faculty of Science and Technology, Hirosaki University, Hirosaki 036-8561, Japan
(Received 22 May 2013; published 29 July 2013)

2D-vectorial equations

A. $\varepsilon > 0$ case

$$\hat{\boldsymbol{\beta}} = \hat{\boldsymbol{\theta}} - \frac{\hat{\boldsymbol{\theta}}}{\hat{\theta}^{n+1}} \quad (\hat{\theta} > 0),$$

$$\hat{\boldsymbol{\beta}} = \hat{\boldsymbol{\theta}} - \frac{\hat{\boldsymbol{\theta}}}{(-\hat{\theta})^{n+1}} \quad (\hat{\theta} < 0),$$

magnification matrix $A_{ij} \equiv \partial \beta^i / \partial \theta_j$

$$(A_{ij}) = \begin{pmatrix} 1 - \frac{1}{\hat{\theta}^{n+1}} + (n+1)\frac{\hat{\theta}_x \hat{\theta}_x}{\hat{\theta}^{n+3}} & (n+1)\frac{\hat{\theta}_x \hat{\theta}_y}{\hat{\theta}^{n+3}} \\ (n+1)\frac{\hat{\theta}_x \hat{\theta}_y}{\hat{\theta}^{n+3}} & 1 - \frac{1}{\hat{\theta}^{n+1}} + (n+1)\frac{\hat{\theta}_y \hat{\theta}_y}{\hat{\theta}^{n+3}} \end{pmatrix}.$$

for $\hat{\theta} > 0$

Axisymmetry enables to diagonalise the magnification matrix as

$$(A_{ij}) = \begin{pmatrix} 1-\kappa-\gamma & 0 \\ 0 & 1-\kappa+\gamma \end{pmatrix} \equiv \begin{pmatrix} \lambda_- & 0 \\ 0 & \lambda_+ \end{pmatrix},$$

$$\lambda_+ = \frac{\hat{\beta}}{\hat{\theta}} = 1 - \frac{1}{\hat{\theta}^{n+1}},$$

$$\lambda_- = \frac{d\hat{\beta}}{d\hat{\theta}} = 1 + \frac{n}{\hat{\theta}^{n+1}}.$$

convergence $$\kappa = 1 - \frac{\lambda_+ + \lambda_-}{2} = \frac{1-n}{2}\frac{1}{\hat{\theta}^{n+1}},$$

shear $$\gamma = \frac{\lambda_+ - \lambda_-}{2} = -\frac{1+n}{2}\frac{1}{\hat{\theta}^{n+1}},$$

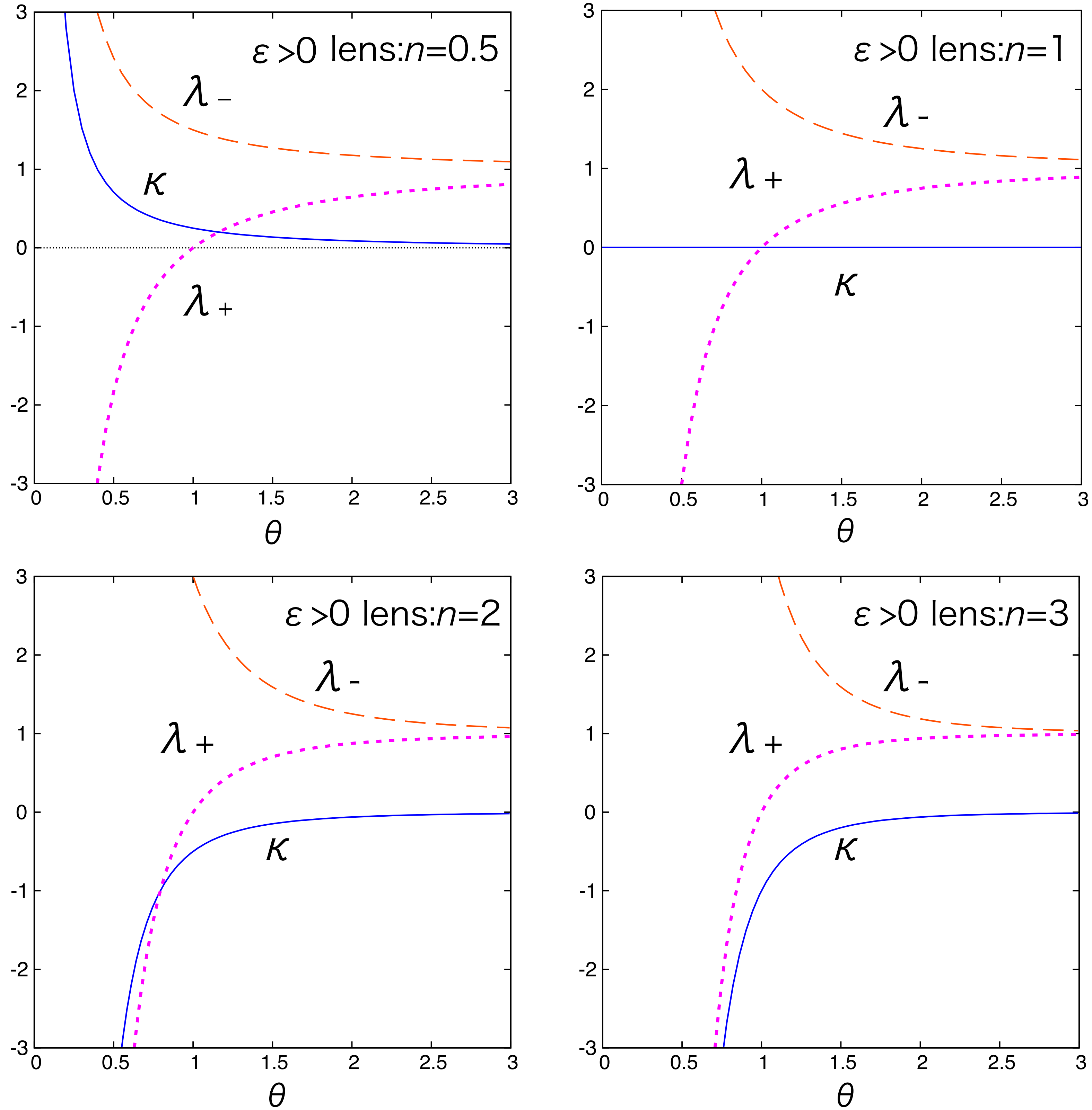

$\lambda_- > \lambda_+$ **tangentially elongated**

B. $\varepsilon < 0$ case

repulsive

like a concave lens

$$\hat{\beta} = \hat{\theta} + \frac{\hat{\theta}}{\hat{\theta}^{n+1}} \quad (\hat{\theta} > 0),$$

$$\hat{\beta} = \hat{\theta} + \frac{\hat{\theta}}{(-\hat{\theta})^{n+1}} \quad (\hat{\theta} < 0).$$

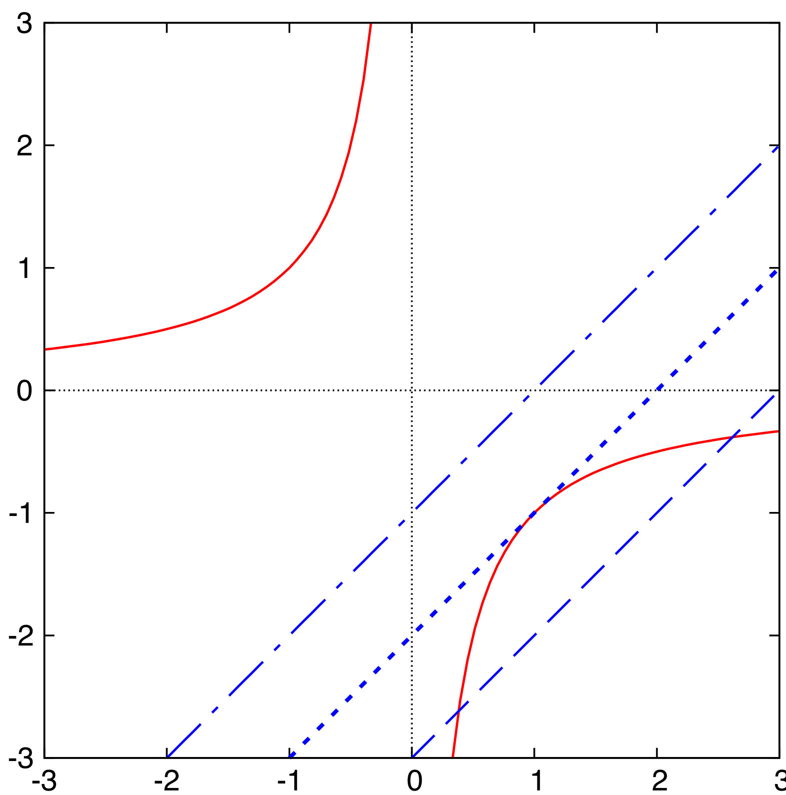

0 images

1 images

2 images

FIG. 3 (color online). Repulsive lens model ($\varepsilon < 0$). Solid curves denote $1/\hat{\theta}^n$ and straight lines mean $\hat{\theta} - \hat{\beta}$. Their intersections correspond to image positions that are roots for the lens equation. There are three cases: No image for a small $\hat{\beta}$ (dot-dashed line), a single image for a particular $\hat{\beta}$ (dotted line), and two images for a large $\hat{\beta}$ (dashed line). The two images are on the same side of the lens object.

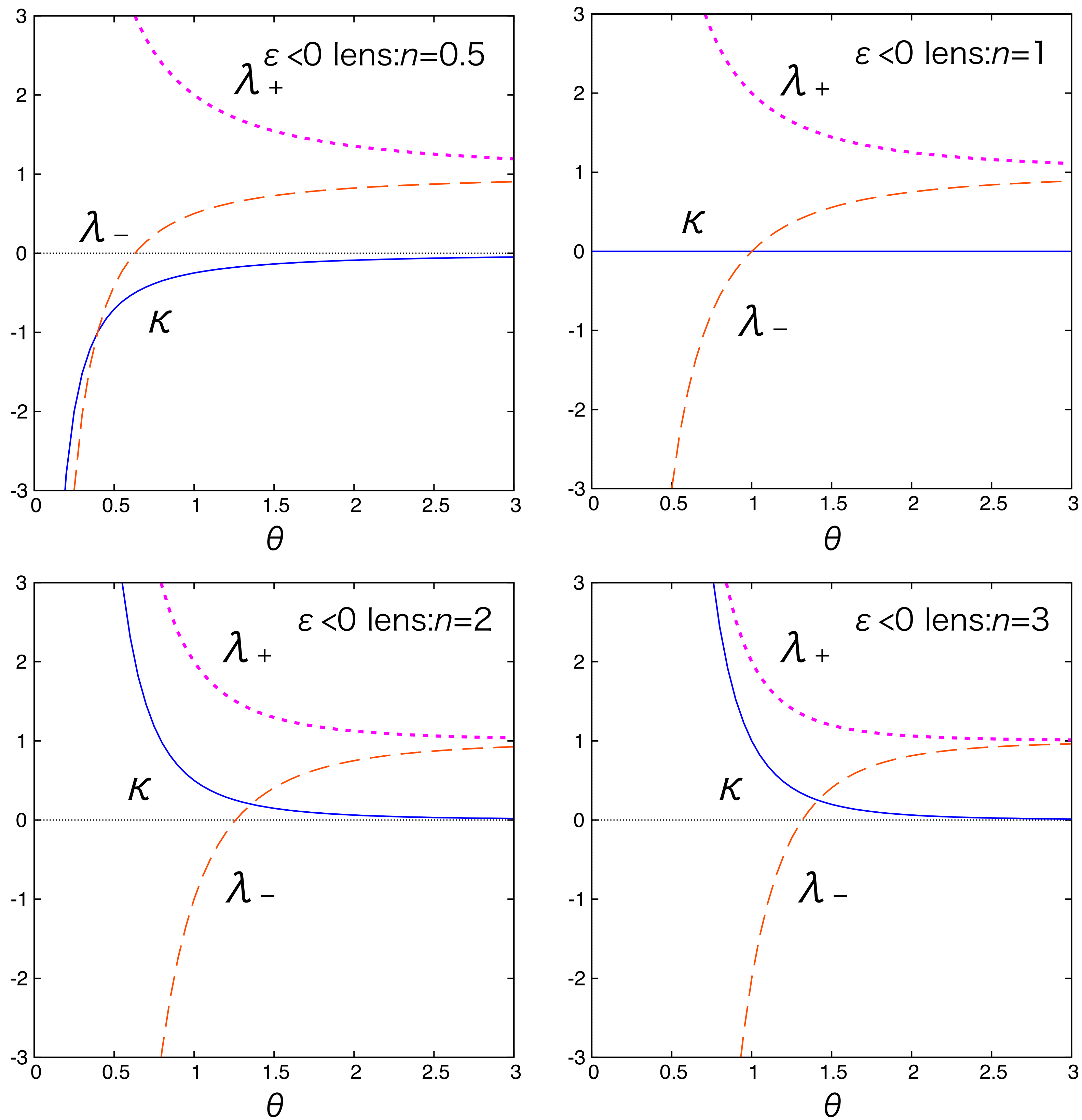

$$\lambda_- < \lambda_+$$

radially elongated

Numerical images

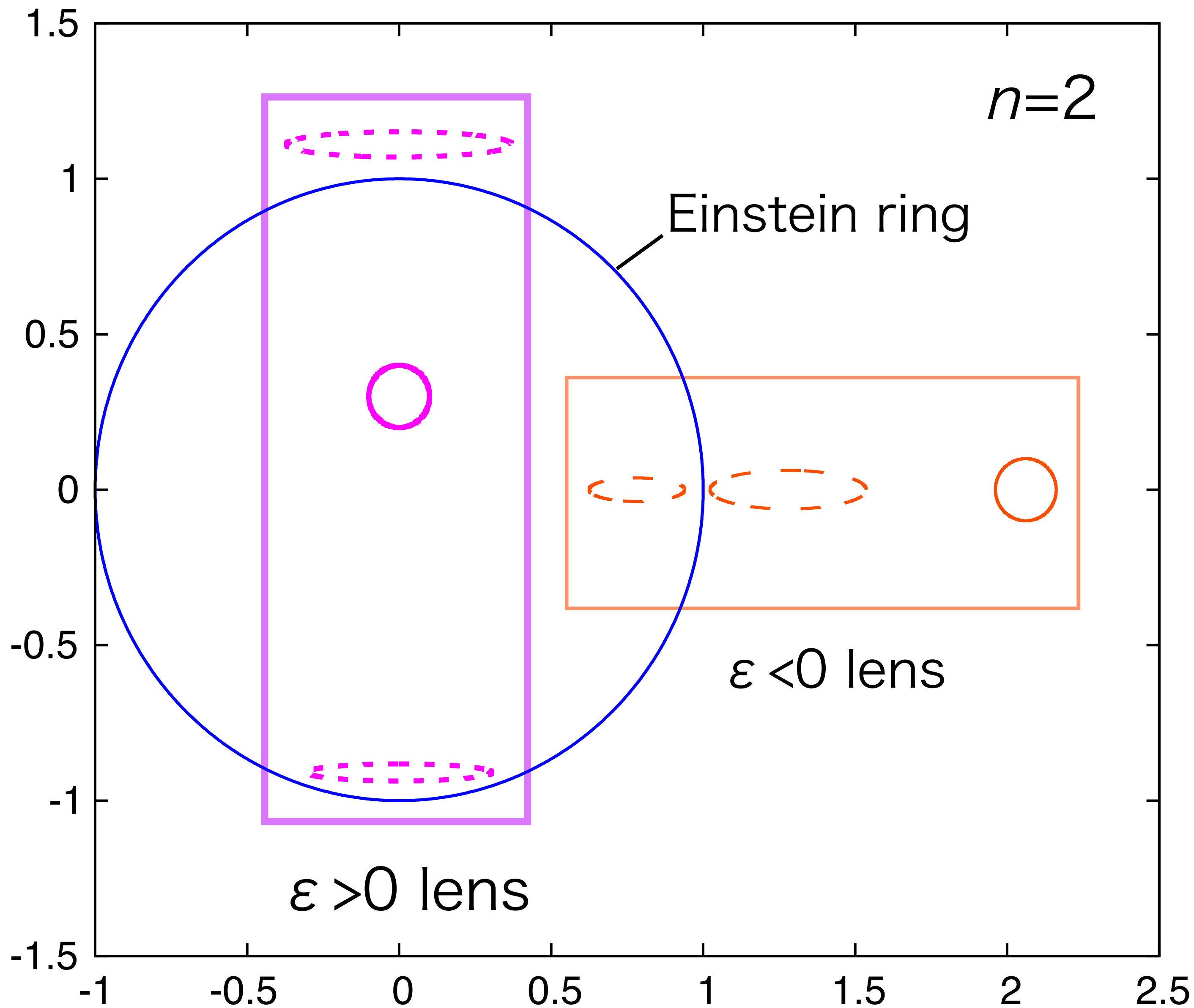

FIG. 2 (color online). Numerical figures of lensed images for attractive ($\varepsilon > 0$) and repulsive ($\varepsilon < 0$) cases. They are denoted by dashed curves. We take $n = 2$. The source for each case is denoted by solid circles, which are located on the horizontal axis and the vertical one for $\varepsilon < 0$ and $\varepsilon > 0$, respectively.

No lens

M > 0

M < 0

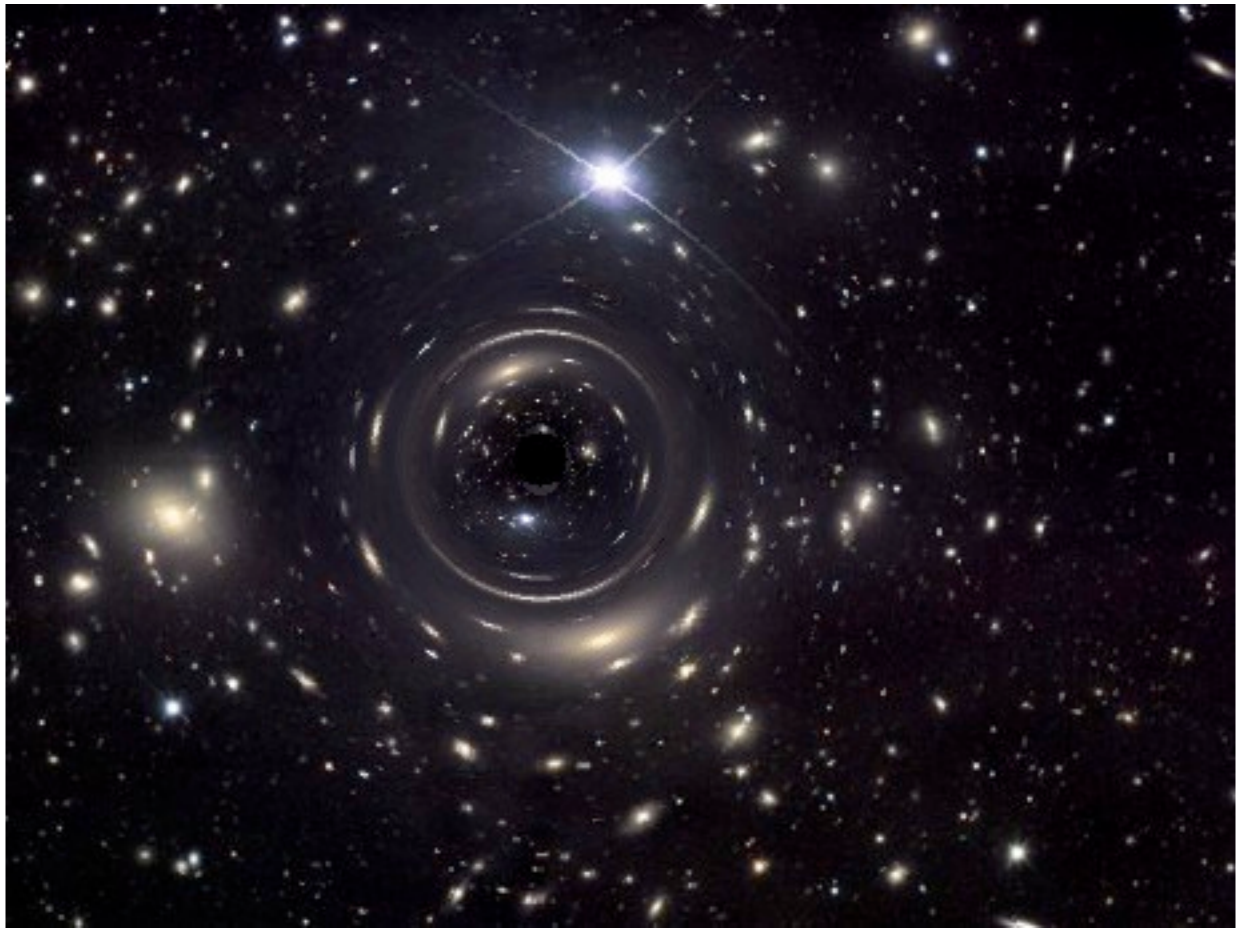

courtesy of Koji Izumi

3) Image motion(micro)

PHYSICAL REVIEW D **89,** 084020 (2014)

Microlensed image centroid motions by an exotic lens object with negative convergence or negative mass

Takao Kitamura, Koji Izumi, Koki Nakajima, Chisaki Hagiwara, and Hideki Asada
Faculty of Science and Technology, Hirosaki University, Hirosaki 036-8561, Japan
(Received 25 July 2013; published 3 April 2014)

Observables in astrometry (e.g. Gaia and JASMINE) are

the centroid position of the light distribution

$$\hat{\boldsymbol{\theta}}_{pc} = \frac{A_1 \hat{\boldsymbol{\theta}}_1 + A_2 \hat{\boldsymbol{\theta}}_2}{A_{tot}},$$

The relative displacement of the image centroid with respect to the source position

$$\delta \hat{\boldsymbol{\theta}}_{pc} = \hat{\boldsymbol{\theta}}_{pc} - \hat{\boldsymbol{\beta}}.$$

Many works for BH and Binary Lens

M. A. Walker, Astrophys. J. **453**, 37 (1995).

M. Miyamoto, and Y. Yoshii, Astron. J. **110**, 1427 (1995).

M. Hosokawa, K. Ohnishi, and T. Fukushima, Astron. J. **114**, 1508 (1997).

N. Safizadeh, N. Dalal, and K. Griest, Astrophys. J. **522**, 512 (1999).

Y. Jeong, C. Han, and S. Park, Astrophys. J. **511**, 569 (1999).

G. F. Lewis, X. R. Wang, Prog. Theor. Phys. **105**, 893 (2001).

H. Asada, Astrophys. J. **573**, 825 (2002).

C. Han, and C. Lee, Mon. Not. Roy. Astron. Soc. **329**, 163 (2002).

EWH case

Y. Toki, T. Kitamura, H. Asada, and F. Abe, Astrophys. J. **740**, 121 (2011).

Convex-type

Star and BH

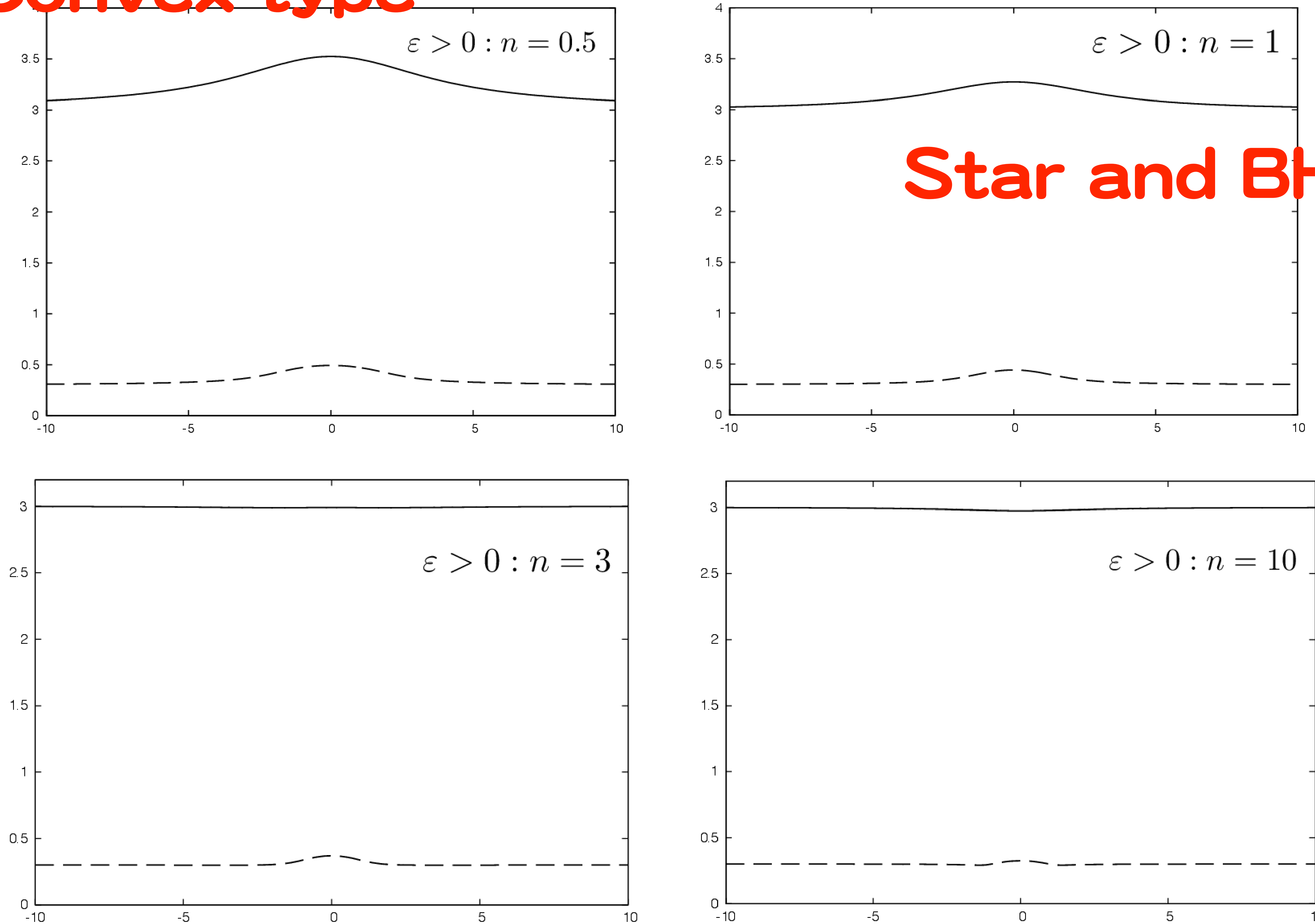

Source motion →

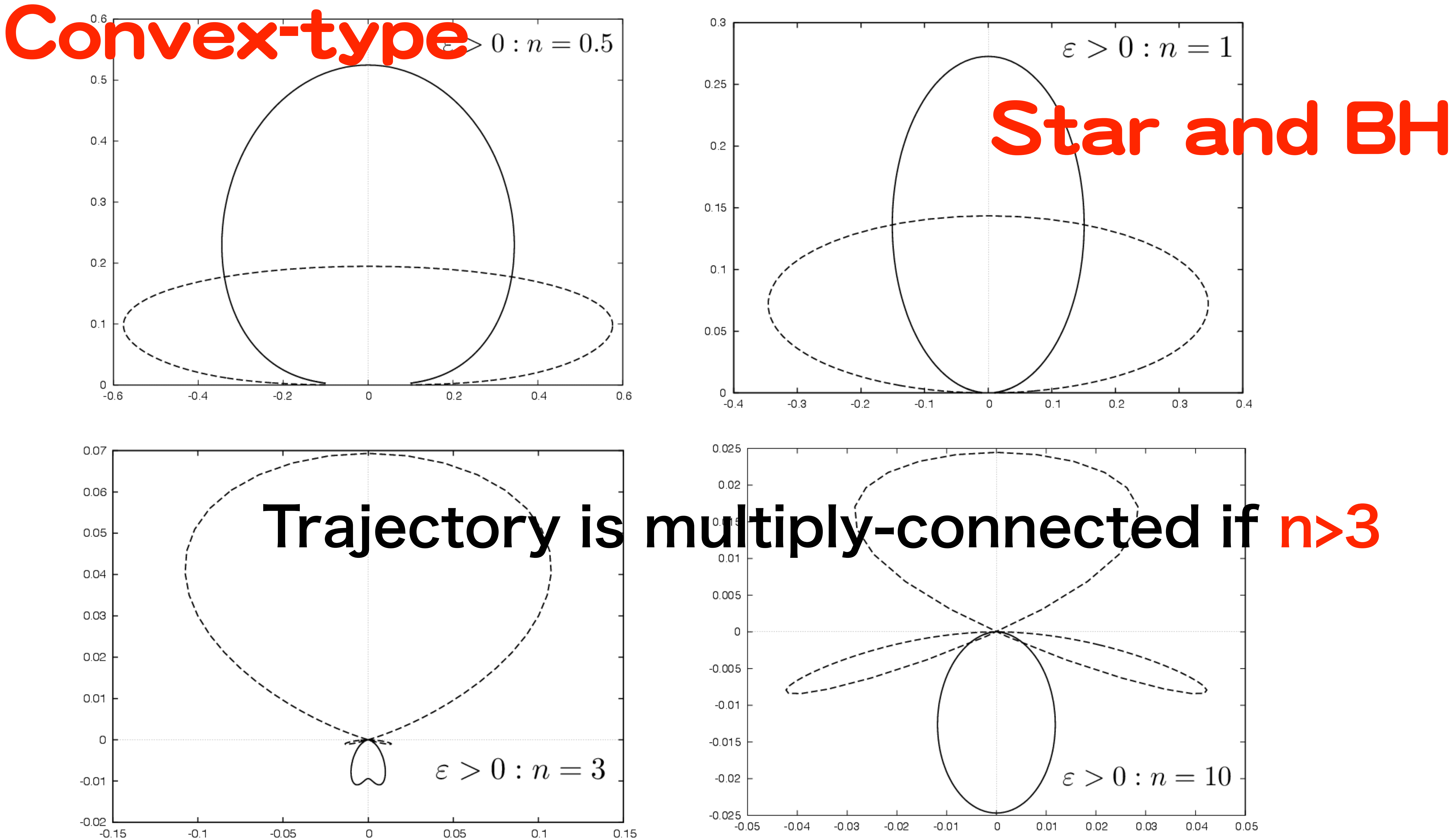

FIG. 3: Centroid shifts $\delta\hat{\boldsymbol{\theta}}_{pc}$ for $\varepsilon > 0$ (convex-type attractive models). The solid and dashed curves correspond to $\hat{\beta}_0 = 3$ and $\hat{\beta}_0 = 0.3$, respectively. The horizontal axis along the source velocity is $\delta\hat{\theta}_{pc,x}$ and the vertical axis is $\delta\hat{\theta}_{pc,y}$. Top left: $n = 0.5$ Top right: $n = 1$. Bottom left: $n = 3$. Bottom right: $n = 10$.

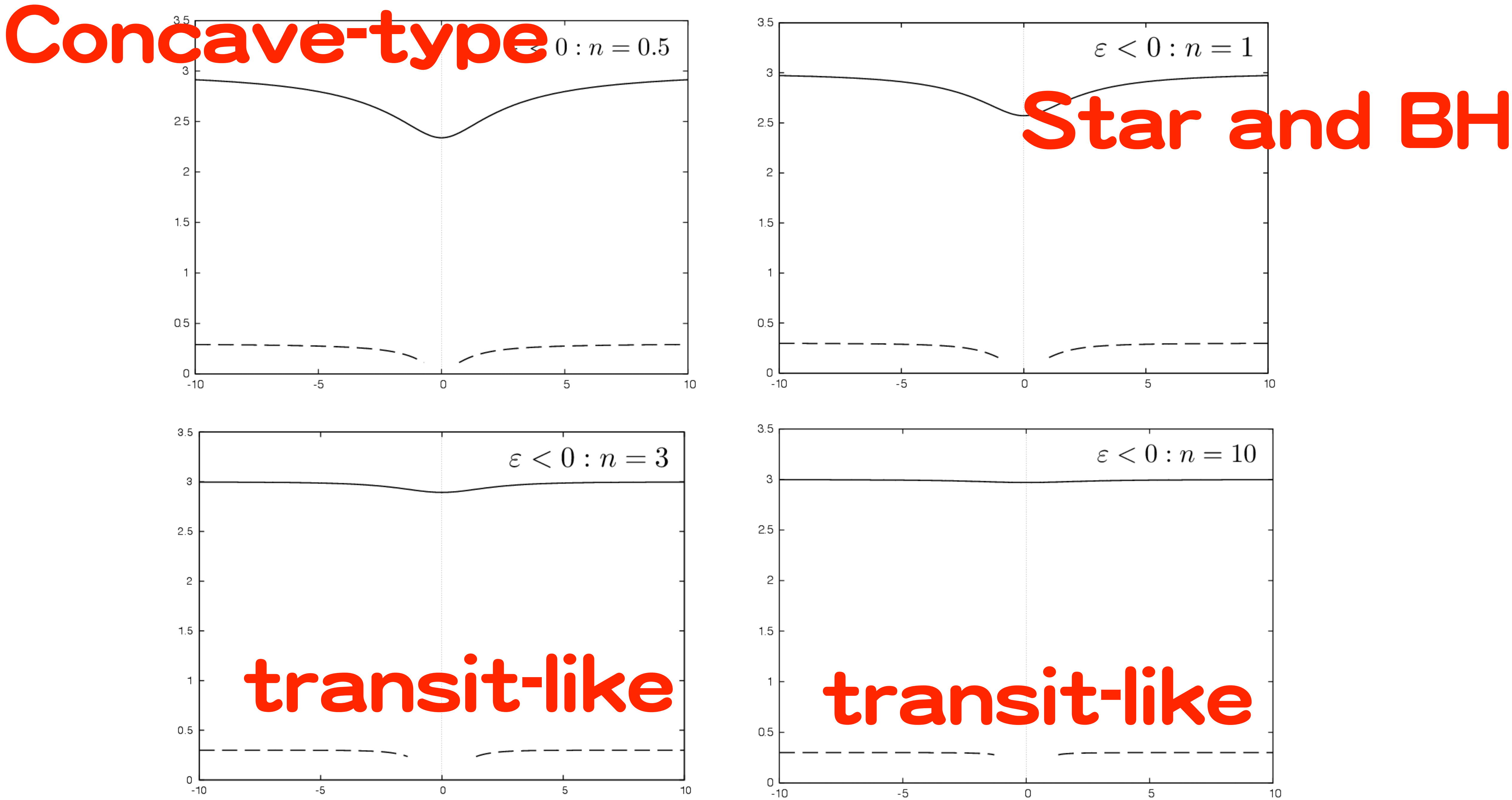

FIG. 6: Centroid motions as $(\hat{\theta}_{pc,x}, \hat{\theta}_{pc,y})$ for $\varepsilon < 0$ (repulsive models). The solid and dashed curves correspond to $\hat{\beta}_0 = 3$ and $\hat{\beta}_0 = 0.3$, respectively. The horizontal axis along the source linear motion is $\hat{\theta}_{pc,x}$ and the vertical axis is $\hat{\theta}_{pc,y}$. The dashed curves do not exist for small $\hat{\beta}$, where no images appear. Top left: $n = 0.5$ Top right: $n = 1$. Bottom left: $n = 3$. Bottom right: $n = 10$.

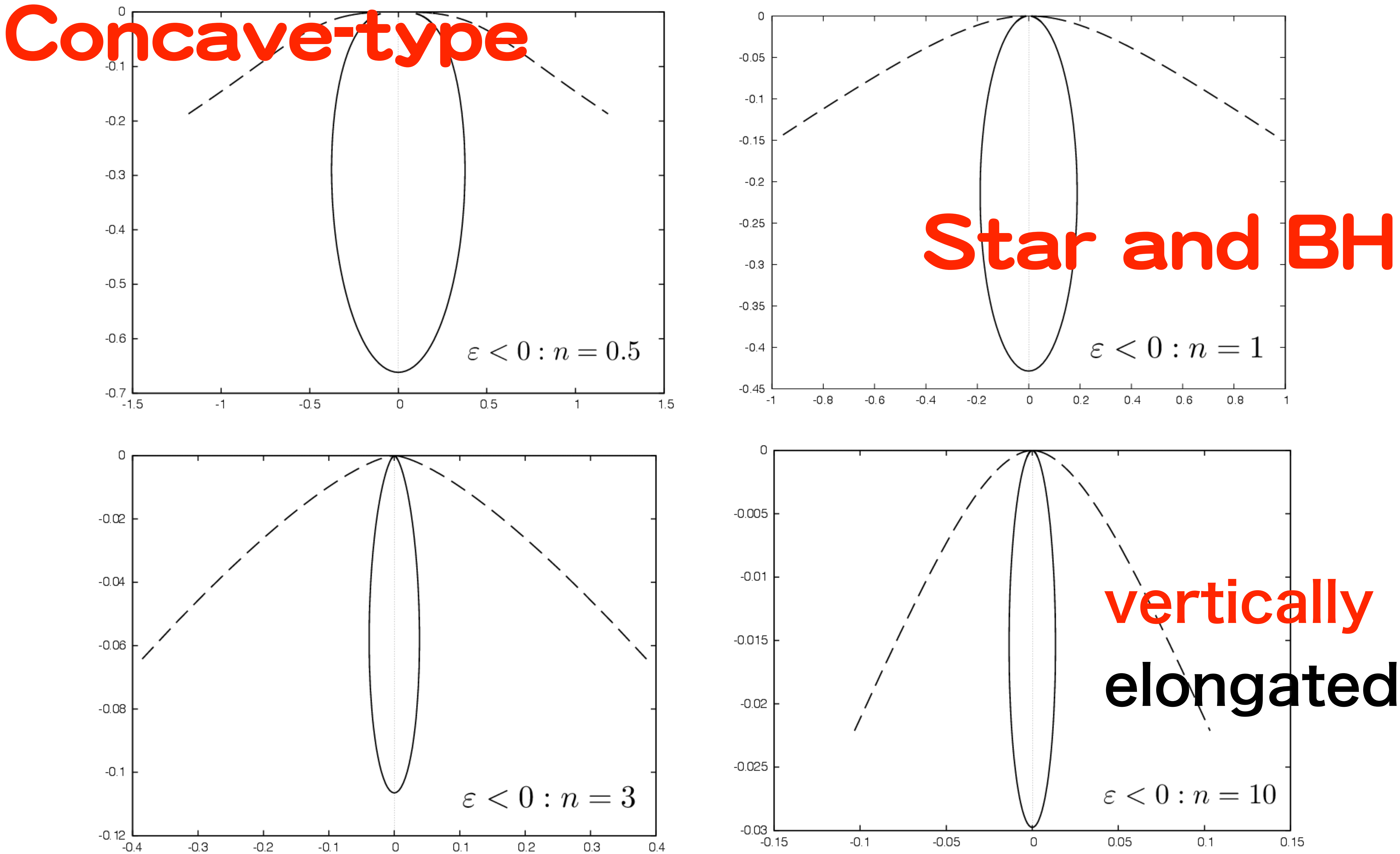

FIG. 7: Centroid shifts $\delta\hat{\boldsymbol{\theta}}_{pc}$ for $\varepsilon < 0$ (concave-type repulsive models). The solid and dashed curves correspond to $\hat{\beta}_0 = 3$ and $\hat{\beta}_0 = 0.3$, respectively. The horizontal axis along the source velocity is $\delta\hat{\theta}_{pc,x}$ and the vertical axis is $\delta\hat{\theta}_{pc,y}$. The dashed curves are not closed, because no images appear for small $\hat{\beta}$. Top left: $n = 0.5$ Top right: $n = 1$. Bottom left: $n = 3$. Bottom right: $n = 10$.

Observational bounds

One example:

THE ASTROPHYSICAL JOURNAL LETTERS, 768:L16 (4pp), 2013 May 1 doi:10.1088/2041-8205/768/1/L16

OBSERVATIONAL UPPER BOUND ON THE COSMIC ABUNDANCES OF NEGATIVE-MASS COMPACT OBJECTS AND ELLIS WORMHOLES FROM THE SLOAN DIGITAL SKY SURVEY QUASAR LENS SEARCH

RYUICHI TAKAHASHI AND HIDEKI ASADA
Faculty of Science and Technology, Hirosaki University, Hirosaki 036-8561, Japan
Received 2013 March 6; accepted 2013 April 4; published 2013 April 17

ABSTRACT

The latest result in the Sloan Digital Sky Survey Quasar Lens Search (SQLS) has set the first cosmological constraints on negative-mass compact objects and Ellis wormholes. There are no multiple images lensed by the above two exotic objects for ~50,000 distant quasars in the SQLS data. Therefore, an upper bound is put on the cosmic abundances of these lenses. The number density of negative-mass compact objects is $n < 10^{-8}(10^{-4})\, h^3$ Mpc^{-3} at the mass scale $|M| > 10^{15}(10^{12})\, M_\odot$, which corresponds to the cosmological density parameter $|\Omega| < 10^{-4}$ at the galaxy and cluster mass range $|M| = 10^{12-15}\, M_\odot$. The number density of the Ellis wormhole is $n < 10^{-4}\, h^3$ Mpc^{-3} for a range of the throat radius $a = 10$–10^4 pc, which is much smaller than the Einstein ring radius.

Key words: cosmology: observations – gravitational lensing: strong

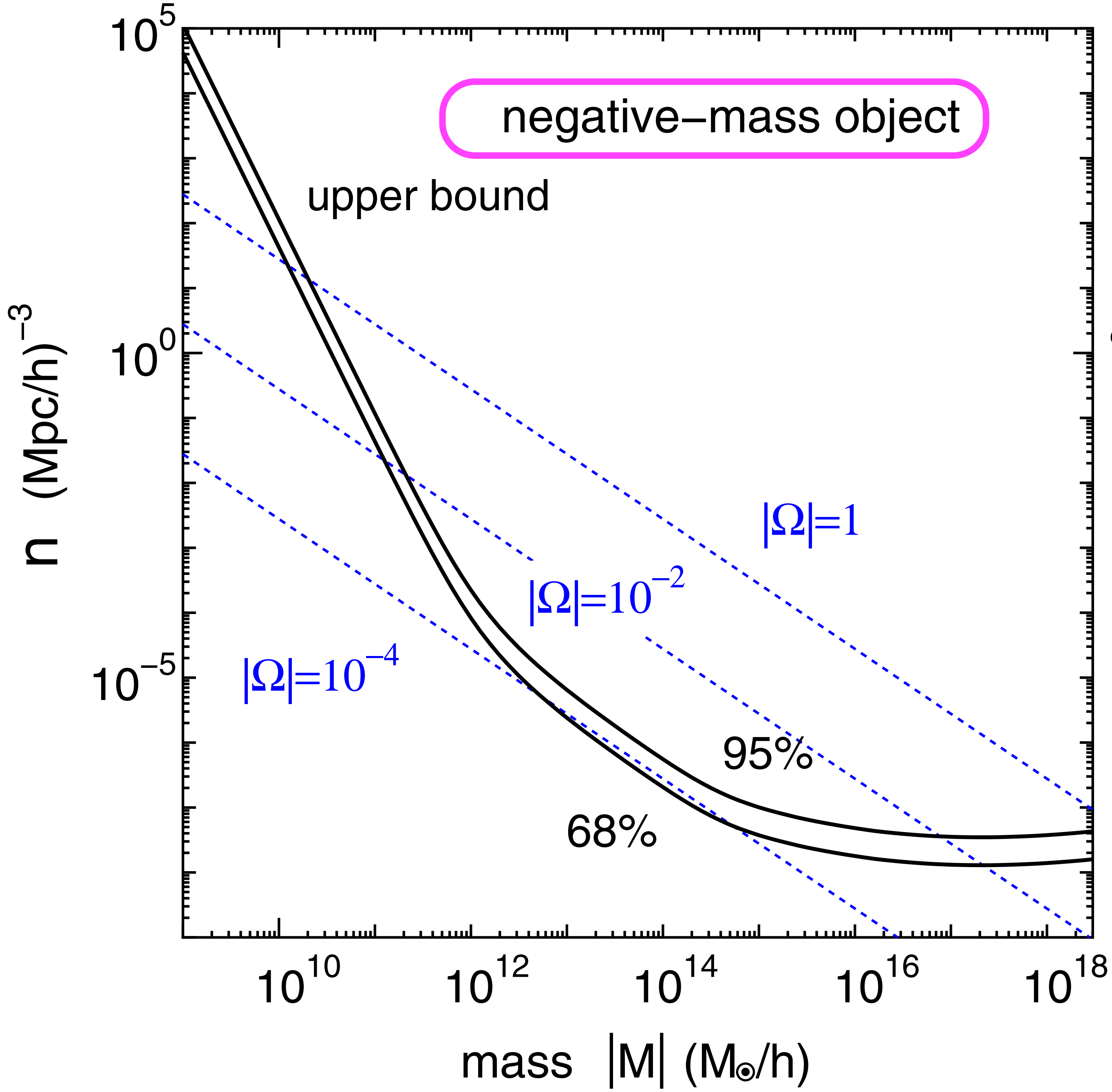

negative–mass object
upper bound
$|\Omega|=1$
$|\Omega|=10^{-2}$
$|\Omega|=10^{-4}$
95%
68%
$n \ (\mathrm{Mpc}/h)^{-3}$
mass $|M|$ ($M_\odot/h$)

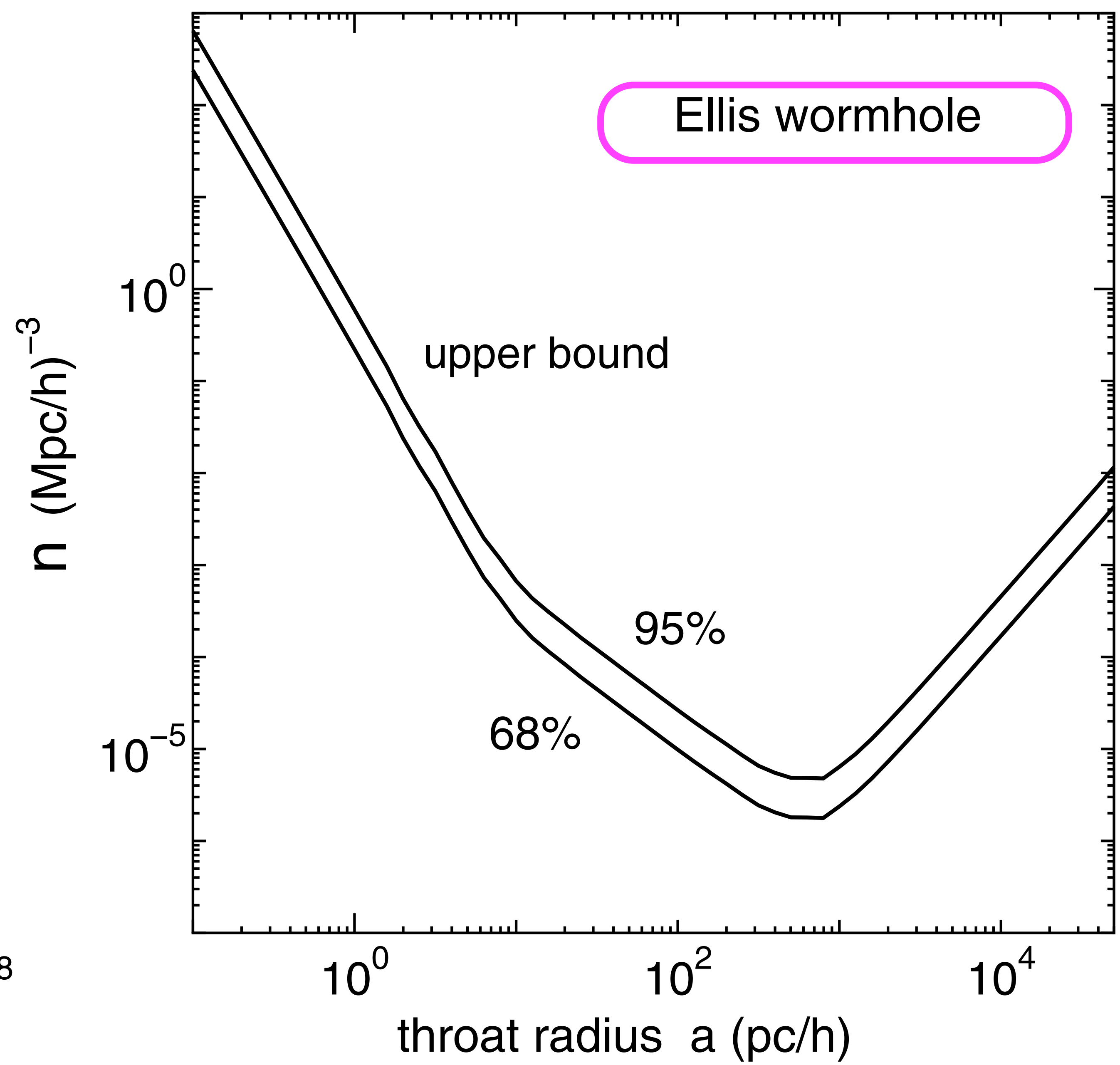

Ellis wormhole
upper bound
95%
68%
$n \ (\mathrm{Mpc}/h)^{-3}$
throat radius a (pc/h)

Conclusion

Womholes and other exotic objects may be a probe of new physics, such as an exotic equation of state of matter/energy.

Brightness anomaly and so on in gravitational lens observations may provide a clue for exotic objects.

We discussed the inverse-power form of the spacetime metric as a phenomenological exotic lens model.

Thank you !

Backup files

Application to cosmology

Cosmic voids: effective $\kappa < 0$

Y. Higuchi, M. Oguri and T. Hamana, MNRAS (2013)

"Measuring the mass distribution of voids with stacked weak lensing"

Numerical simulations for near-future surveys

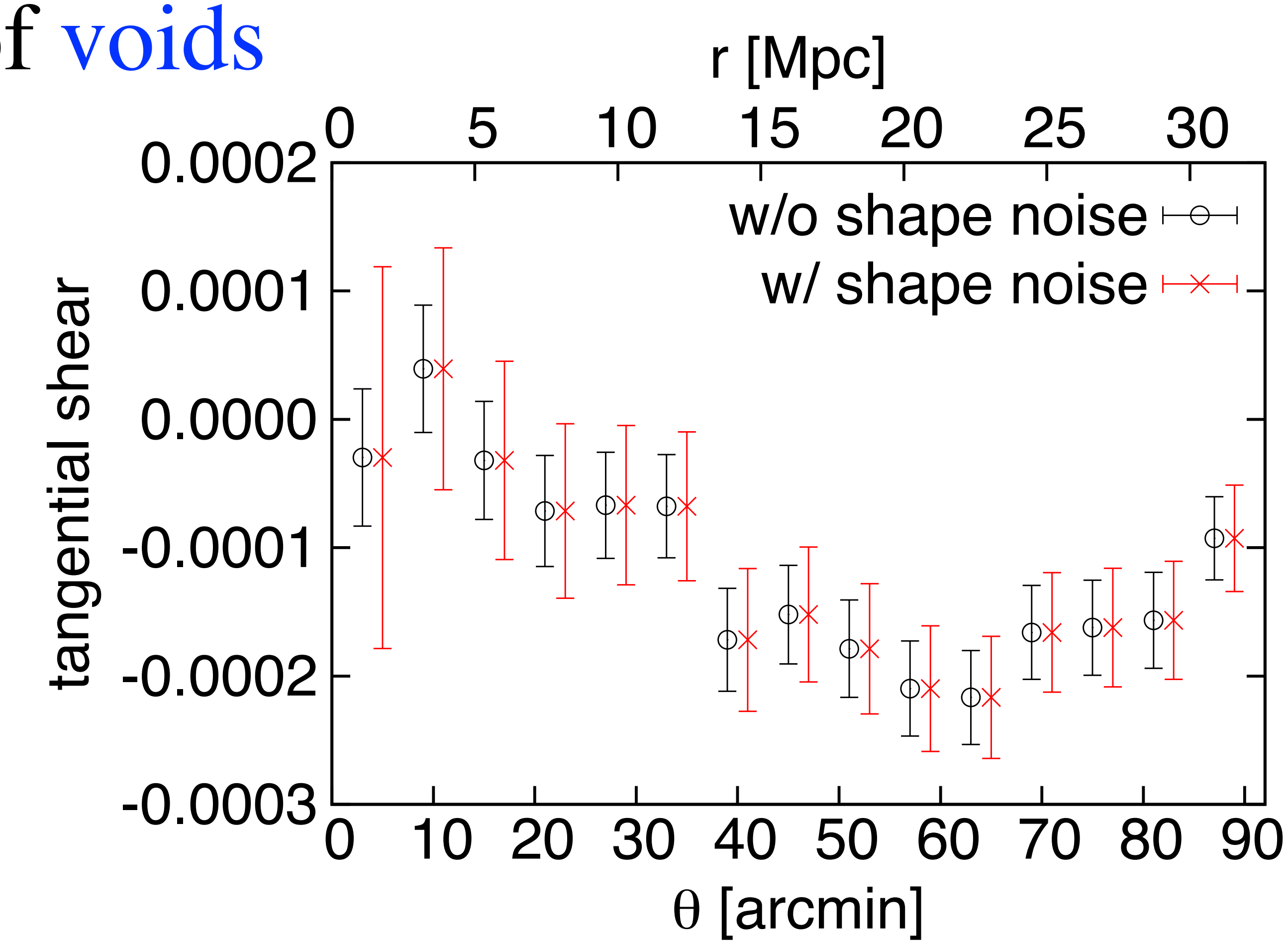

"First measurement of gravitational lensing by cosmic voids in SDSS", Melchior et al., ArXiv:1309.2045

Concluding remarks

Exotic lens models suggest
unusual observational features.

They might be used
for searching (or constraining)
exotic matter/energy/gravity.

Dark matter and Dark energy
play a role in cosmology.

Is there another (3rd) dark component
in the universe ?

TABLE II: Einstein radii and model parameters for Bulge and LMC lensings. θ_E is the angular Einstein radius, R_E is the Einstein radius, and $\bar{\varepsilon}$ and n are the two model parameters. $D_S = 8kpc$ and $D_L = 4kpc$ are assumed for Bulge. $D_S = 50kpc$ and $D_L = 25kpc$ are assumed for LMC.

	Bulge		LMC	
$\theta_E(mas)$	$R_E(km)$	$\frac{\bar{\varepsilon}}{R_E^n}$	$R_E(km)$	$\frac{\bar{\varepsilon}}{R_E^n}$
10^{-3}	6.0×10^5	1.0×10^{-11}	3.7×10^6	1.0×10^{-11}
10^{-2}	6.0×10^6	1.0×10^{-10}	3.7×10^7	1.0×10^{-10}
10^{-1}	6.0×10^7	1.0×10^{-9}	3.7×10^8	1.0×10^{-9}
1	6.0×10^8	1.0×10^{-8}	3.7×10^9	1.0×10^{-8}
10	6.0×10^9	1.0×10^{-7}	3.7×10^{10}	1.0×10^{-7}
10^2	6.0×10^{10}	1.0×10^{-6}	3.7×10^{11}	1.0×10^{-6}
10^3	6.0×10^{11}	1.0×10^{-5}	3.7×10^{12}	1.0×10^{-5}

TABLE III: Einstein radius crossing times for Bulge and LMC lensings. t_E is the Einstein radius crossing time. $D_S = 8kpc$ and $D_L = 4kpc$ are assumed for Bulge. $D_S = 50kpc$ and $D_L = 25kpc$ are assumed for LMC. $v_T = 220km/s$ is assumed for Bulge and LMC. In this table, the Einstein radius is calculated by $R_E = v_T \times t_E$ from the definition of the Einstein radius crossing time. Here, the input is $t_E \sim 10^{-3} - 10^3(day)$, namely $1(min.) - 3(yr.)$.

$t_E(day)$	$R_E(km)$	$\frac{\bar{\varepsilon}}{R_E^n}$ [Bulge]	$\frac{\bar{\varepsilon}}{R_E^n}$ [LMC]
10^{-3}	1.9×10^4	3.1×10^{-13}	5.0×10^{-14}
10^{-2}	1.9×10^5	3.1×10^{-12}	5.0×10^{-13}
10^{-1}	1.9×10^6	3.1×10^{-11}	5.0×10^{-12}
1	1.9×10^7	3.1×10^{-10}	5.0×10^{-11}
10	1.9×10^8	3.1×10^{-9}	5.0×10^{-10}
10^2	1.9×10^9	3.1×10^{-8}	5.0×10^{-9}
10^3	1.9×10^{10}	3.1×10^{-7}	5.0×10^{-8}

Raychaudhuri's equation for null geodesics

$$\dot{\hat{\theta}} = -\frac{1}{2}\hat{\theta}^2 - 2\hat{\sigma}^2 + 2\hat{\omega}^2 - T_{\mu\nu}U^\mu U^\nu$$

$$T\mu\nu U^\mu U^\nu \geq 0$$

Null Energy Condition

But, exotic objects (e.g. wormholes) may violate Null Energy Condition.

Ricci focusing may be negative, while Weyl focusing is positive.

[N.B., Wormholes without exotic matter in Einstein-Gauss-Bonnet-Dilaton gravity, Kanti+, PRL (2011)]